FRACTIONAL OPERATORS AND VARIATIONS

APPLIED TO STEFAN PROBLEMS

By

KATRINA CHRISTEL SABOCHICK

A dissertation submitted in partial fulfillment of
the requirements for the degree of

DOCTOR OF PHILOSOPHY

WASHINGTON STATE UNIVERSITY
Department of Mathematics and Statistics

DECEMBER 2023

To the Faculty of Washington State University:

The members of the Committee appointed to examine the dissertation of KATRINA CHRISTEL SABOCHICK find it satisfactory and recommend that it be accepted.

Sergey Lapin, Ph.D., Co-Chair

Lynn Schreyer, Ph.D., Co-Chair

Daryl DeFord, Ph.D.

ACKNOWLEDGMENT

First, I would like to thank my advisor Dr. Sergey Lapin for taking me on as a student and helping to guide me through the end of my Ph.D. I would also like to thank Dr. Lynn Schreyer for providing advice and support during my time at WSU, and Dr. Kevin Vixie for showing me a side of graduate student life beyond academics.

I am forever grateful to my peers Paula Kimmerling, Matthew Gaddis, Jakob Streipel, Ryan Whitehead, and Emily Lewis for their encouragement, advice, laughter, and support. This thesis would not exist without them.

A special thank you to my parents, Carol and George, for supporting my dream of graduate education and helping from afar.

Finally, I am forever grateful for my husband Ryan, who traveled with me across the country to help me pursue my goals. I look forward to our adventures to come.

FRACTIONAL OPERATORS AND VARIATIONS

APPLIED TO STEFAN PROBLEMS

Abstract

by Katrina Christel Sabochick, Ph.D.
Washington State University
December 2023

Co-Chairs: Sergey Lapin and Lynn Schreyer

In this thesis, we present a model for the free boundary Stefan problem. We begin with outlining the problem and its complexities, motivating the need for a numerical method. Then we introduce fractional operators, exploring various characteristics to narrow down the proper operator that will apply to the Stefan problem. We then outline our model, using the Caputo fractional derivative with a finite difference discretization and the SOR method to solve numerically. Our results are presented for different parameters such as latent heat and temperature. We end with suggestions for further work on our model.

keywords : Free boundary problem, PDEs, numerical analysis, Stefan problems, Caputo derivatives, fractional operators

TABLE OF CONTENTS

Page

ACKNOWLEDGMENT iii

ABSTRACT iv

LIST OF TABLES vii

LIST OF FIGURES viii

CHAPTER

1 INTRODUCTION 1
1.1 Stefan Problems 1
1.2 Fractional Time Derivatives 2

2 THE STEFAN PROBLEM 4
2.1 Foundations and Definitions 4
2.1.1 Thermodynamics 4
2.2 Derivation of the One-Phase Stefan Problem 5
2.2.1 The Stefan Condition 7
2.2.2 The One-Dimensional Problem 8
2.2.3 Assumptions 9
2.3 Characteristics of the One-Phase Stefan Problem 10
2.3.1 Existence and Uniqueness 10
2.3.2 Similarity Solution 13
2.4 The Two-Phase Stefan Problem 16
2.5 The Two-Dimensional Stefan Problem 18
2.5.1 General Overview 18
2.5.2 Stability of Two-Dimensional Perturbations 19
2.6 Conclusions 21

3 FRACTIONAL OPERATORS 22
3.1 Fractional Derivatives: Overview 23
3.1.1 Preliminary Definitions 23
3.1.2 The Riemann-Liouville Fractional Integral 24
3.1.3 The Riemann-Liouville Fractional Differential Operator 24
3.1.4 The Caputo Fractional Differential Operator 25
3.2 Properties of the Caputo Fractional Derivative 26
3.3 The Caputo Laplace Transform 29
3.3.1 Advantages and Disadvantages 32
3.4 Conclusions 32

4 THE STEFAN CAPUTO MODEL 34
4.1 The One-Dimensional Model 34
4.1.1 Finite Difference Scheme 36
4.1.2 SOR Method 38
4.2 The Two-Dimensional Model 39

5 RESULTS 41
5.1 One-Dimensional Model 41
5.1.1 Alpha Values 41
5.1.2 Initial Temperatures 43
5.1.3 Latent Heat 44
5.2 Two-Dimensional Model 46
5.2.1 Alpha Values 46
5.2.2 Latent Heat 49
5.2.3 Heat Source Variation 51
5.2.4 Summary 54

6 CONCLUSIONS 55

REFERENCES 58

APPENDIX

A Block Diagram for One-Dimensional Algorithm 60

B Code for One-Dimensional Stefan Caputo Model 61

C Code for Two-Dimensional Stefan Caputo Model 65

LIST OF TABLES

-Table		Page
2.1	The latent heat of fusion (melting) for a few select substances, from [13]. . .	5
5.1	Summary of parameter comparisons for the one-dimensional model.	45
5.2	Summary of parameter comparisons for the two-dimensional model.	54

LIST OF FIGURES

Figure Page

2.1 Depiction of 1D slab with two phases. Adapted from [16]. 6

2.2 The rectangular domain E_T, on the (x, t) axis. 11

2.3 Relationship between β and St, from [23] 15

2.4 General schematic for the 2-D Stefan problem. Adapted from [23] 18

4.1 Graph of enthalpy function $H(u)$ 36

4.2 Uniform mesh grid 37

5.1 Graph for $\alpha \to 1$ showing the movement of the free boundary over time . . . 42

5.2 Comparison between the free boundary for $\alpha \to 1$ and $ln(y) = 0.5ln(t) + b$. 42

5.3 The movement of the phase boundary for varying alpha values 43

5.4 The movement of the phase boundary for varying heat source temperatures . 44

5.5 The movement of the phase boundary for various latent heat values. 45

5.6 3D plot of the two-dimensional Stefan Caputo model for $\alpha = 0.5$ 47

5.7 Heat map of the 2D region at fixed time $k = 20$ 47

5.8 3D plots of the two-dimensional model for varying α values 48

5.9 3D plots of the two-dimensional model for varying latent heat values 50

5.10 3D plots of the two-dimensional model for varying heat source temperatures 51

5.11 3D plot showing the model with a central heat source radiating outward . . 52

5.12 3D plot showing the model with a concentrated central heat source 53

5.13 3D plot showing the model with an edge heat source 53

A.1 Block diagram 60

Dedication

This dissertation is dedicated to my husband Ryan

CHAPTER ONE

INTRODUCTION

1.1 Stefan Problems

A Stefan problem is a type of free boundary problem for a system of PDEs, where the phase-change boundary can move with time. The problem consists of two unknowns.

- a set Ω (generally $\subset \mathbb{R}^n$)
- a function $u : \Omega \to \mathbb{R}$

The aim is to find solutions (Ω, u) where u satisfies a boundary condition, as well as a free boundary condition on $\partial\Omega$.

A Stefan problem is a particular type of boundary problem that deals with phase transitions. The classical problem describes the changes in the boundary between two phases of a material - for example, the melting of ice to water.

Take a semi-infinite slab of ice, and impose a constant heat source on one end. The semi-infinite length of the slab means that the melting boundary will never reach the other end - instead, it will eventually reach an equilibrium.

The system involves solving heat equations for each region (liquid and solid), with various constants and boundary conditions applied. At the boundary between the two phases, the temperature is the phase change temperature - in the case of ice, this value is 0°C, when ice melts to water.

We also add in the Stefan condition, a function of quantities evaluated on either side of the boundary, expressing the local velocity of this boundary. This is because at the phase

change interface, the solution to the PDEs may have discontinuities, so the Stefan condition is required to obtain closure and make the problem well-posed.

This one-phase Stefan problem has been explored using a variety of methods and boundary conditions, but there are some guaranteed similarities.

We start with a few basic definitions for the system - $s(t)$ represents the phase boundary, $u(x,t)$ is the temperature at space x and time t, and the enthalpy function. Enthalpy is a state function that is the sum of the internal energy and the product of pressure and volume. This function changes over time in the system, and has different constants for different materials. We will explore these constant further in Chapter 2.

One element of this is that we end up with two unknowns - the location of the phase boundary, and the temperature. While the simplest version of the one-phase, one-dimensional Stefan problem can be solved analytically, real-world applications require a numerical approach.

1.2 Fractional Time Derivatives

We can use fractional operators to help with our solution - specifically, the Caputo fractional derivative, though we will explore other fractional operators as well to motivate our choice.

The Caputo fractional derivative is useful for the model, since we need to take into account interactions at the free boundary in the past. In vague terms, one can think of the Caputo derivative as having a "memory," rather than treating each time iteration as a standalone calculation.

We will construct our model using a finite difference scheme for the fractional derivative.

We begin by choosing an initial temperature and boundary condition. Then, for each time iteration we look for the position of the phase change boundary using known (or estimated) values of temperature and enthalpy from previous iterations, taken from a uniform mesh grid of space and time. After using successive over-relaxation (SOR) to solve our system,

we can then use a simple comparison to find our boundary, computing the fractional time derivative and enthalpy to give us a single value. If that value is positive, then the ice has not yet melted - if it's zero or negative, we have switched to liquid. This uniform mesh grid allows to not only track the changes in temperature, but also track the location of the moving boundary. Our goal is to create a model that will solve the simple Stefan problem, and then use that model to explore various enthalpy constants and initial conditions for the system. We will aim to solve this problem for both one and two dimensions, and explore the results when we vary the heat source location and temperatureerature for various parameters.

Once we have established our model, we will run through iterations varying α values for the fractional derivative, as well as other material parameters, for both one and two dimensions.

CHAPTER TWO

THE STEFAN PROBLEM

2.1 Foundations and Definitions

In general, a free boundary problem is a partial differential equation (PDE) in which there are two unknowns:

- a set Ω (generally $\subset \mathbb{R}^n$)
- a function $u : \Omega \to \mathbb{R}$

The problem consists of finding solutions (Ω, u), where u satisfies a boundary condition, as well as a free boundary condition on $\partial\Omega$.

A *Stefan Problem* is a particular type of boundary problem that deals with phase transitions - for example, the melting of ice to water over time. The boundary between the ice and water will move as the ice melts, shifting over time before potentially reaching an equilibrium.

2.1.1 Thermodynamics

The movement of this boundary comes with a unique challenge. Fixed boundaries must have equal heat flux on each side, but a moving interface includes energy for a phase change.

The energy required for a phase change is known as *latent heat*. Latent heat acts as an energy source/sink at a moving interface, whereas sensible heat is the heat that causes a change in temperature.

Enthalpy, in thermodynamics, is the sum of a system's internal energy and the product of pressure and volume, $H = U + pV$, where U is the internal energy, p is pressure, and V is the volume of the system. Enthalpy of fusion, or latent heat of fusion (shortened to 'latent heat'), is the change in enthalpy that results from energy (heat) to a quantity of a substance to change its state from solid to liquid.

For example, if we aim to melt 1 kg of ice at 0°C, the ice will absorb 334.55 kJ of energy to melt with no change in temperature. The liquid phase has a higher internal energy than the solid phase, so energy must be absorbed by the solid to change its state.

The latent heat of fusion differs for various materials. The table below highlights some latent heat values (for kJ/kg) of a few common substances.

Material	Latent Heat of Fusion (kJ/kg)
Carbon dioxide	184
Lead	23
Mercury	11.4
Nickel	293
Silver	105
Ice (water)	334

Table 2.1 The latent heat of fusion (melting) for a few select substances, from [13].

2.2 Derivation of the One-Phase Stefan Problem

We will begin with a simple example of a one-dimensional Stefan problem, consisting of the melting of ice to water [16].

A slab of solid ice occupies the region $x \in (0, a)$. The temperature $u(x, t)$ satisfies that heat equation

$$\rho c \frac{\partial u}{\partial t} = \frac{\partial}{\partial x}\left(k \frac{\partial u}{\partial x}\right)$$

where ρ, c, and k are density, heat capacity/specific heat, and thermal conductivity, respectively. We will mostly be treating these values as constants throughout our work.

Suppose the slab is a uniform temperature of u_0, and the right boundary $x = a$ is insulated so that no heat escapes. A heat source of temperature u_m is then applied to the boundary $x = 0$. We expect the ice to melt and become liquid in some neighborhood of $x = 0$.

Given the two phases - solid and liquid - we must solve the heat equation in both areas of the domain Ω, with different specific heats and conductivity, separated by the boundary $s(t)$. The position of $s(t)$ is unknown, but the phase change does occur at a known temperature u_m (for example, $O°C$ for ice to water). Note that for simplicity, we will ignore the small changes in volume that occur during transition.

We should expect that $u_L \geq u_m$ in the liquid region $\Omega_1 = \Omega \cap \{x < s(t)\}$, and $u_S \leq u_m$ in the solid region $\Omega_2 = \Omega \cap \{x > s(t)\}$.

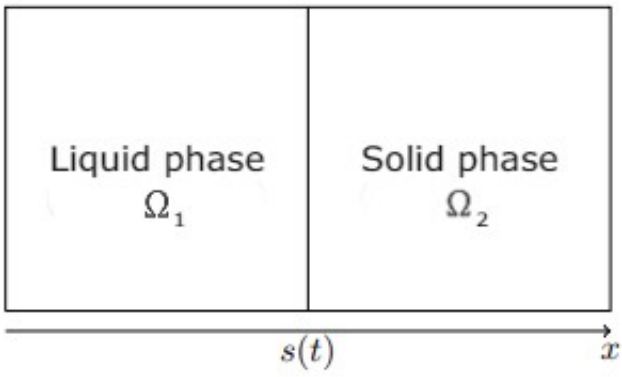

Figure 2.1 Depiction of 1D slab with two phases. Adapted from [16].

For a solution to the classical Stefan problem, we must solve the heat equation for different regions, and the evolving phase change interface (or simply 'interface') requires a boundary condition called the Stefan condition, which we will now derive. A deeper exploration of the Stefan condition is available in [16].

2.2.1 The Stefan Condition

We will now derive the Stefan condition, adapted from [16]. Physically, we expect that temperature is continuous at $s(t)$, such that

$$\lim_{x \to s(t)^+} u_S = \lim_{x \to s(t)^-} u_L = u_m.$$

As we move from time $t = t_0$ to, say, $t = t_1$, the position of the interface will change to $s(t_1) > s(t_0)$. Then, a portion of the interface of volume $S \times (s(t_1) - s(t_0))$ (where S is the area) has melted, and a quantity of heat Q has been released.

$$Q = S(s(t_1) - s(t_0))\rho L, \tag{2.1}$$

where ρ is the density, and L is the specific latent heat, from [16]. Then we have the heat flux for each region, defined as

$$\phi_L = -K_L \frac{\partial u_L}{\partial x} \tag{2.2}$$

$$\phi_S = -K_S \frac{\partial u_S}{\partial x}. \tag{2.3}$$

Here, K_i is the conductivity ($i = L$ for liquid, $i = S$ for solid), and we assume that $u_i(x,t) \in C^1$, where $D_x u_l = \frac{\partial u}{\partial x}$. Then, since energy is conserved, we assume that the total heat absorbed in equation (2.1) sums to the following:

$$Q = \int_{t_0}^{t_1} \int_A -K_L \frac{\partial u_L}{\partial x}(s(\tau),\tau) \cdot \mathbf{x} - K_S \frac{\partial u_S}{\partial x}(s(\tau),\tau) \cdot (x\mathbf{x}) dA d\tau \tag{2.4}$$

Here, $\mathbf{x}$ is the unit vector in the x direction. Integrating over the spatial coordinates and equating equations (2.1) and (2.4), we are left with

$$(s(t_1) - s(t_0))\rho L = \int_{t_0}^{t_1} \left[-K_L \frac{\partial u_L}{\partial x}(s(\tau),\tau) + K_S \frac{\partial u_S}{\partial x}(s(\tau),\tau) \right] d\tau. \tag{2.5}$$

Simplifying and taking the limit as $t_1 \to t_0$, we get

$$\rho L \lim_{t_1 \to t_0} \frac{s(t_1) - s(t_0)}{t_1 - t_0} = \lim_{t_1 \to t_0} \frac{1}{t_1 - t_0} \int_{t_0}^{t_1} \left[-K_L \frac{\partial u_L}{\partial x}(s(\tau), \tau) + K_S \frac{\partial u_S}{\partial x}(s(\tau), \tau) \right] d\tau. \quad (2.6)$$

From here, we can apply the Mean Value Theorem for integrals. Letting $f(k) \equiv -K_L u_x(s(k), k) + K_S u_x(s(k), k)$, we can simplify this equation, and as f is continuous since $u \in C^1$, we get

$$L\rho s'(t_1) = \lim_{t_1 \to t_0} \times (t_1 - t_0) f(k)$$
$$L\rho s'(t_1) = f(t_1)$$

Since t_1 was arbitrary, we get that $L\rho s'(t) = f(t)$. This presents a boundary condition known as the *Stefan condition*:

$$k \frac{\partial T}{\partial x}\Big|_{x>s(t)} - k \frac{\partial T}{\partial x}\Big|_{x<s(t)} = \rho L \frac{ds}{dt} \quad (2.7)$$

2.2.2 The One-Dimensional Problem

Now that we have established the Stefan condition, we can state the problem. Again, we assume that any volume change is negligible, and that the solid region has a constant temperature. Thus we need to find the distribution of temperature in the liquid region, and the position of the interface $s(t)$ - this is called a one-phase problem.[16]

For simplicity, let $\alpha_i = \dfrac{K_i}{c_i \rho}$. Then the problem can be stated as thus:

$$
\begin{aligned}
\frac{\partial u}{\partial t} = \frac{K_L}{c_L \rho}\frac{\partial^2 u}{\partial x^2} &= \alpha_L \frac{\partial^2 u}{\partial x^2}, && 0 < x < s(t), t > 0, \\
u(0,t) &= f(t), && t > 0 \\
u(x,0) &= 0, && 0 \leq x \leq a \\
L\rho \frac{ds}{dt} &= -K_L \frac{\partial u}{\partial x}, && x = s(t), \\
s(0) &= 0 \\
u(s(t),t) &= 0 \\
u(x,t) &= 0, && \forall t, \quad x \geq s(t)
\end{aligned}
\tag{2.8}
$$

At the boundary of $x = 0$, we could apply a number of conditions - here, we will use $f(t) = 1$.

2.2.3 Assumptions

Before we proceed further, let us briefly summarize some assumptions that have been made. When we used the heat flux Q to calculate the Stefan condition, we are assuming that it satisfies Fourier's law, such that

$$\phi = -K\frac{\partial u}{\partial x}$$

This requires that the heat flux is only due to thermal conductivity. If we allowed for the liquid to flow, there would be an additional contribution from convection.

We have also assumed that the density ρ is continuous across the interface $s(t)$ - if we allowed for ρ to change as the ice melts, we would have nonzero convective heat flux. Instead, we assume that the change in density is negligible.

2.3 Characteristics of the One-Phase Stefan Problem

2.3.1 Existence and Uniqueness

For the purpose of numerical analysis, we show that the problem is well-posed, i.e.:

1. The solutions exists
2. The solution is unique
3. The solution depends continuously on the data.

The first two requirements are satisfied by the same theorem. We will then establish the third requirement through use of the maximum principle, though this will be explored further for higher dimensional problems later on. This theorem is a special case of the work presented in [9].

Theorem 2.3.1. *For $u(0,t) = f(t)$ where $f(t) \in C^1$ and $u(x,0)$ is a constant, there exists a unique solution $\{u(x,t), s(t)\}$ of (2.8) for $t < \infty$.*

Next, we can establish monotonicity, but first we will state and prove the weak maximum principle. The maximum principle is a generalization of a very simple property often seen in early calculus - the maximum of a function f will occur at the endpoints of a closed interval $[a,b]$, if $f'' > 0$. Extending the principle to any domain Ω and other differential inequalities can help establish information about a differential equation, even before finding the solution itself, since we can confirm that the maximum is achieved on the boundary $\partial\Omega$.

Theorem 2.3.2 (The Weak Maximum Principle)**.** *Suppose the function $u(x,t)$ satisfies the inequality*

$$L(u) \equiv \frac{\partial^2 u}{\partial x^2} - \frac{\partial u}{\partial t} \geq 0$$

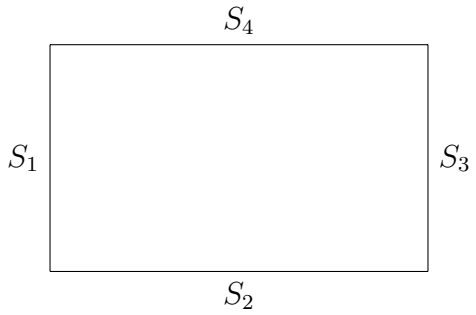

Figure 2.2 The rectangular domain E_T, on the (x, t) axis.

in the region $E_T = \{(x,t) : 0 < x < l(t), 0 < t \leq T\}$. *Then, the maximum value of* u *on* $\overline{E_t}$ *must occur on boundaries* S_1, S_2, *or* S_3, *where*

$$S_1 : \{x = 0 : 0 \leq t \leq T\},$$
$$S_2 : \{0 \leq x \leq l(t) : t = 0\},$$
$$S_3 : \{x = l(t) : 0 \leq t \leq T\}$$
$$S_4 : \{0 < x < l : t = T\}.$$

Proof. First, we want to ensure that the maximum value is attained on the boundary. We will do so by proving a preliminary lemma.

Lemma 2.3.3. *Assume that* $u(x,t) \in C^2$, *and satisfies that differential inequality* $L(u) > 0$ *in* E_T. *Then the maximum value of* u *cannot be attained at the interior of* $\overline{E_T}$.

Proof. Assume that the maximum value of u is attained at interior point $P = (x_1, t_1) \in \overline{E}$. Since P is a critical point, the derivative $u_t = 0$, and since it's a maximum then $u_{xx}(x_0, t_0) \leq 0$.

However, this would mean that $L(u) \leq 0$, which contradicts the differential inequality. Therefore, the maximum of u cannot be attained at an interior point. □

Now that we've established the maximum occurring on the boundary, let us use contradiction to show that it can only be attained on S_1, S_2, or S_3.

Let M be the largest value of u occurring on S_1, S_2, S_3, and assume that there exists a point $P = (x_1, t_1)$ where $u(P) = M_1 > M$.

Define the following function:

$$\omega(x) = \frac{M_1 - M}{2l^2}(x - x_1)^2 \tag{2.9}$$

Additionally, let $\upsilon(x,t) \equiv u(x,t) + \omega(x)$.

On the boundaries S_1, S_2, S_3, we know that $u \leq M$ and $0 < x < l$. Therefore, we have the inequality

$$\upsilon(x,t) \leq M + \frac{M_1 - M}{2} < M_1. \tag{2.10}$$

Then at the interior point (x_1, t_1), we have

$$\upsilon(x_1, t_1) = u(x_1, t_1) + 0 = M_1 \tag{2.11}$$

and in the region E_T, we are left with

$$L(\upsilon) = L(u) + L(\omega) = L(u) + \frac{M_1 - M}{l^2} > 0 \tag{2.12}$$

From the inequality in (2.10) and the interior point condition (2.11), we can conclude that the maximum must be obtained on the interior of E, or in the upper boundary:

$$S_4 : \{0 < x < l : t = T\} \tag{2.13}$$

However, from (2.3.3), we know that we cannot have a maximum on the interior, since we have the differential inequality from (2.12). If instead we end up with the maximum on S_4, then we have the following implication:

$$\frac{\partial^2 \upsilon}{\partial x^2} \leq 0 \implies \left.\frac{\partial \upsilon}{\partial t}\right|_{t=T} < 0 \tag{2.14}$$

This tells us that v must have a larger value when $t < T$, which is a contradiction. Therefore, our assumption that $u(x_1, t_1) > M$ is incorrect.

□

Now we have the tools we need prove that the one-phase and one-dimensional Stefan problem is well-posed.

Theorem 2.3.4. *If there is a solution $\{u, s(t)\}$ to (2.8) for $t < \sigma$ for finite σ, then $x = s(t)$ is monotone non-decreasing.*

Proof. The Weak Maximum Principle tells us that $u(x,t) \geq 0$ when $0 < x < s(t)$. Because the phase change temperature at $x = s(t)$ is $u = 0$, the rate of change in temperature at the $x = s(t)$ must be ≤ 0. Thus we have that $\frac{ds}{dt} \geq 0$, so $s(t)$ is monotone non-decreasing. □

2.3.2 Similarity Solution

While most of our research will focus on numerical work of the Stefan problem, we will now briefly explore the second-order ordinary differential equation and accompanying analytical solution that can help expand our understanding, and confirm our numerical model for certain parameters. Portions of this work, along with more theoretical work on the one-dimensional Stefan problem, can be found in [16] and [23].

Normalizing the dependent variables and nondimensionalizing our definition from (2.8), we can rewrite:

$$\begin{aligned} \mathrm{St}\frac{\partial u}{\partial t} &= \frac{\partial^2 u}{\partial x^2}, && 0 < x < s(t), \quad t > 0 \\ u &= 1 && x = 0, \quad t > 0 \\ u = 0, \qquad -\frac{\partial u}{\partial x} &= \frac{ds}{dt} && x = s(t), \quad t > 0 \\ s(0) &= 0 \end{aligned} \tag{2.15}$$

Here, the non-dimensionalized parameter St is known as the *Stefan number*[1], defined as

$$\mathrm{St} = \frac{c(u_1 - u_m)}{L}$$

, where u_m is the melting temperature, and u_1 is the current temperature.

The Stefan number measures the relation between the sensible heat and latent heat. As a reminder, the sensible heat is the energy required to raise the temperature, while the latent heat is the energy required to undergo the phase change.

Then we wish to find a similarity solution of (2.15), where we have that for some constant β,

$$s(t) = \beta\sqrt{t} \tag{2.16}$$

$$u(x,t) = f(\eta) \tag{2.17}$$

where $\eta = \frac{x}{\sqrt{t}}$. Then we have the free boundary problem

$$\begin{aligned} \frac{d^2 f}{d\eta^2} + \frac{\mathrm{St}}{2}\eta\frac{df}{d\eta} = 0, &\qquad 0 < \eta < \beta \\ f = 1, &\qquad \eta = 0 \\ f = 0, \frac{df}{d\eta} = -\frac{\beta}{2}, &\qquad \eta = \beta \end{aligned} \tag{2.18}$$

where we have boundary conditions on a second-order ODE and β must be determined for the solution, and

$$f(\eta) = 1 - \frac{\mathrm{erf}(\eta\sqrt{\mathrm{St}}/2)}{\mathrm{erf}(\beta\sqrt{\mathrm{St}}/2)} \tag{2.19}$$

where $\mathrm{erf}\, z$ is the Gauss error function, and β satisfies the transcendental equation

[1]Some authors define the Stefan number as the reciprocal of this.

$$\frac{\sqrt{\pi}\beta e^{St\beta^2/4}\,\mathrm{erf}(\beta\sqrt{St}/2)}{2\sqrt{St}} = 1. \tag{2.20}$$

The parameter β and the Stefan number St are related, with asymptotic limits approximated:

$$\beta \sim \begin{cases} \sqrt{2} & \text{as } St \to 0 \\ \frac{2}{\sqrt{St}}\sqrt{\log\left(\frac{St}{\sqrt{\pi}}\right)} & \text{as } St \to \infty \end{cases} \tag{2.21}$$

Given St, we can determine β and the evolution of the free boundary $s(t)$. For this example, the entire slab has melted when $s(t) = 1$, so the (dimensionless) time it takes to melt is $1/\beta^2$. Reversing the nondimensionalization gives approximations for the melting time t_m:

$$t_m \sim \begin{cases} \frac{\rho L a^2}{2k(u_1 - u_m)} & \text{if } St << 1 \\ \frac{\rho c a^2}{4k\log(St/\sqrt{\pi})} & \text{if } St >> 1. \end{cases} \tag{2.22}$$

When St is small, the melting is mainly dependent on the latent heat required, and the one phase solution gives us a quick way to find the location of the boundary.

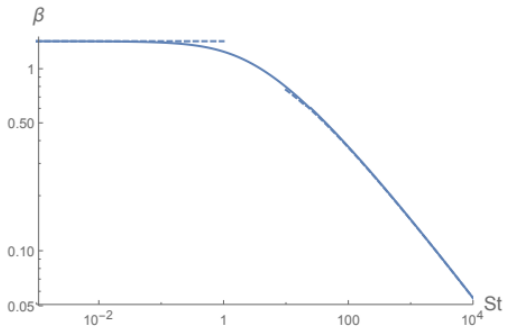

Figure 2.3 Relationship between β and St, from [23]

For example: Suppose we melt a block of ice, where the heat source on one face is 10. The parameters are $L = 334$ kJ/kg and $c = 4.2$ kJ/kgK, which results in $St \approx 0.125$, and a β value calculated from (2.20) only off from $\sqrt{2}$ by 1%.

2.4 The Two-Phase Stefan Problem

Our work up until this point has been focused on the one-phase Stefan problem: that is, when the initial temperature of the slab is equal to the phase change temperature, requiring us to solve the heat equation only in the melted region of our domain.

If, however, we allow the initial temperature of the slab to be below the phase change temperature, the problem becomes more complex. For the two-phase version of the (dimensionless) Stefan problem, we have the following, adapted from [23]:

$$
\begin{aligned}
\mathrm{St}\frac{\partial u}{\partial t} &= \frac{\partial^2 u}{\partial x^2} && 0 < x < s(t), \quad t > 0 \\
\frac{\mathrm{St}}{\kappa}\frac{\partial u}{\partial t} &= \frac{\partial^2 u}{\partial x^2} && s(t) < x < 1, \quad t > 0 \\
u &= 1 && x = 0, t > 0 \\
\frac{\partial u}{\partial x} &= 0 && x = 1, t > 0 \\
u = 0, \qquad K\left[\frac{\partial u}{\partial x}\right]^{+} - \left[\frac{\partial u}{\partial x}\right]^{-} &= \frac{ds}{dt} && x = s(t), \quad t > 0 \\
u = -\theta, \qquad s &= 0 && t = 0
\end{aligned}
$$

with new parameters

$$
\kappa = \frac{c_1 k_2}{c_2 k_1} \qquad K = \frac{k_2}{k_1} \qquad \theta = \frac{u_m - u_0}{u_1 - u_m}
$$

where c_i denotes the specific heat and k_i is the thermal conductivity, with $0 < x < s(t)$ for $i = 1$, $s(t) < x < 1$ for $i = 2$.

The difficulty of this problem requires us to solve numerically - however, there are a few special cases where analytic progress can be made. If we allow $\mathrm{St} \to 0$, the two heat equations become quasi-steady. If we integrate directly, we end up with

$$u(x,t) = \begin{cases} 1 - \frac{x}{s(t)} & 0 < x < s(t) < 1 \\ 0 & 0 < s(t) < x < 1 \end{cases} \tag{2.23}$$

and applied to the Stefan condition, we get

$$\frac{ds}{dt} = \frac{1}{s}$$

so that $s(t) = \sqrt{2t}$, which matches the one-phase solution we obtained above where $\beta = \sqrt{2}$.

However, this approximate solution does not satisfy the initial condition $u = -\theta$ (except where $u_0 = u_m$, reducing the problem to one-phase), so additional adjustments must be made by adding a boundary layer in which u shifts from $-\theta$ to (2.15).

2.5 The Two-Dimensional Stefan Problem

2.5.1 General Overview

The two-dimensional Stefan problem is depicted below. Note that to avoid confusion, u_1 and u_2 denote the temperatures in the solid and liquid regions, respectively, satisfying the two-dimensional heat equations.

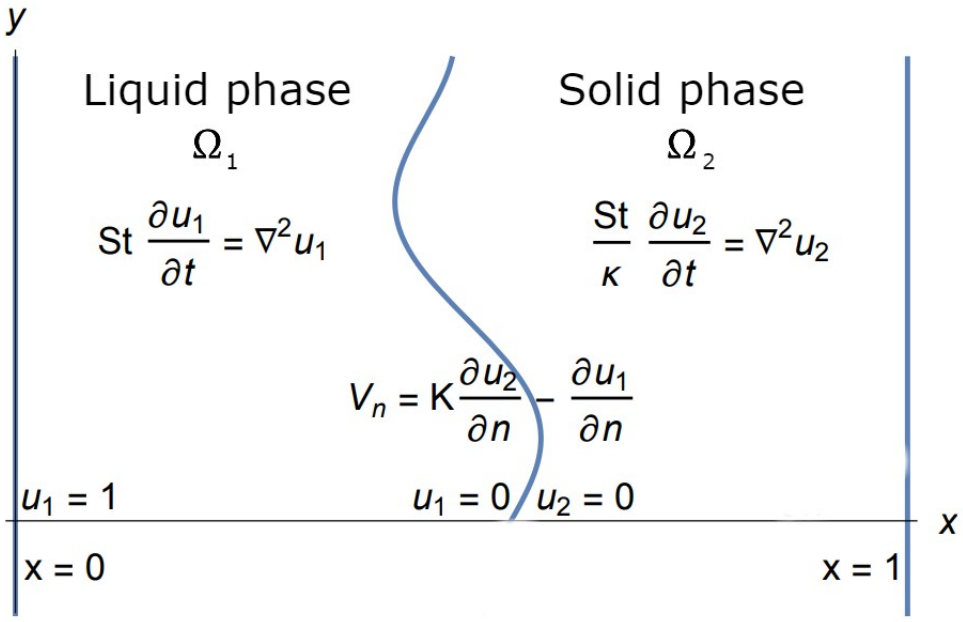

Figure 2.4 General schematic for the 2-D Stefan problem. Adapted from [23]

Unlike the one-dimensional problem, the free boundary is now an xy curve, where $u_1 = u_2 = u_m$. The Stefan condition

$$V_n = K\frac{\partial u_2}{\partial n} - \frac{\partial u_1}{\partial n} \tag{2.24}$$

relates the normal velocity, V_n, of the free boundary to the normal derivative of the temperature in either region. Additionally, we need to specify the initial temperature over the entire domain, as well as initial position of the free boundary.

As with the one-dimensional problem, we can simplify if we take St$\to$ 0, so that the temperature u can satisfy Laplace's equation in the two regions. In doing so, the resulting problem closely resembles a Hele-Shaw flow, a prominent problem in fluid mechanics first presented in [22].

2.5.2 Stability of Two-Dimensional Perturbations

Now that we have established the two-dimensional Stefan problem, we will briefly analyze the stability of the perturbations. First, we will make a few assumptions to simplify the calculations, from [23]. We will allow the limit St$\to$ 0, which as stated above reduces the problem to a Hele-Shaw flow. We will also focus our attention on the one-phase Stefan problem, where $u_2 \equiv u_m \equiv 0$ (i.e., the solid region is already at the phase change temperature).

We will also assume that the phase change boundary is moving at a constant speed V, with a constant temperature gradient $-\lambda$, before being perturbed. Thus the (normalized) temperature can be written as

$$u(x, y, t) = -\lambda(x - Vt) + \tilde{u}(x, y, t), \tag{2.25}$$

where the position of the free boundary is $x = Vt + \xi(y, t)$. Next, we want to linearize the problem with respect to $\tilde{u}$ and ξ. Since the material is solid in the region $x > Vt$ and liquid where $x < Vt$, λ should be positive.

For the leading-order term, the Stefan condition represents the relation between the speed V and the gradient, $V = \lambda$. Thus we have

$$\nabla^2 \tilde{u} = 0, \qquad x < Vt \tag{2.26}$$

$$\tilde{u_1} - \lambda\xi = 0, \qquad x = Vt \tag{2.27}$$

$$-\frac{\partial \tilde{u}}{\partial x} = \frac{\partial \xi}{\partial t}, \qquad x = Vt. \tag{2.28}$$

We wish to find a separable solution, where we have the following

$$\tilde{u}(x, y, t) = Ae^{\sigma t + iky + k(x - Vt)} \tag{2.29}$$

$$\xi(y, t) = Be^{\sigma t + iky}. \tag{2.30}$$

Here, k is the spatial frequency of the wave (also referred to as the "wave number), and σ is the growth rate. We chose this representation so that Laplace's equation is satisfied, and so $\tilde{u}$ and ξ decay as $x \to -\infty$.

The two equations for the phase chase boundary can be represented in linear form for A and B, such that

$$\begin{bmatrix} 1 & -\lambda \\ k & \sigma \end{bmatrix} \begin{bmatrix} A \\ B \end{bmatrix} = \begin{bmatrix} 0 \\ 0 \end{bmatrix}$$

Nontrivial solutions require the determinant of the coefficient matrix to be 0, so we need $\sigma - (-\lambda k) = 0$, and thus $\sigma = -\lambda k = -Vk$. If we are melting a solid into liquid, so that V is positive, then $\sigma < 0$ for all k, which tells us that the phase boundary is stable.

But if we instead freeze a liquid into a solid - when V is negative - the boundary will be unstable instead. In this situation, we must have that $\lambda < 0$ - in other words, the liquid temperature is actually lower than the melting point, so the liquid is supercooled.

When V is negative, we also have that the growth rate is unbounded, so arbitrarily small perturbations of the phase change boundary can cause extremely large changes quickly, particularly for very large spatial frequencies k. This is a result of an ill-posed problem, as the behavior of the solution does not change continuously based on the data. This characteristic makes the liquid-to-solid problem as stated here nearly impossible to solve numerically. (In fact, this difference is intuitive - an ice cube will generally melt with a smooth face, while water undergoing the freezing process can crystallize with a very irregular phase boundary.)

In general, variations of the temperature gradients may cause the problem to be unstable

and ill-posed, and often require additional physical parameters. Modern approaches for liquid-to-solid problems may also incorporate a "mush region" where the two phases coexist. Further information about the mush region in Stefan problems can be found in [17].

2.6 Conclusions

In exploring the derivation of the one-phase Stefan problem in one and two dimensions, we have shown that only within very specific conditions can the problem be solved analytically. Numerical methods are needed to solve the problem for two phases or two dimensions.

Additionally, the assumptions that we used in our analytic solutions restrict us a great deal. For the classical problem, the heat flow was determined using Fourier's law, but in many systems the heat flow equation is not given by the law (see [3]).

Our motivation now is to find a numerical approach that can be generalized to various materials and sizes, for both one and two dimensions. We seek a highly flexible model that can be adjusted to fit the needs of the system. The general technique of using the finite difference method and various boundary conditions has been applied in the past. We hope to find a process that is comparable to analytic solutions, can be extended to more complex parameters, and has a reasonable runtime.

CHAPTER THREE

FRACTIONAL OPERATORS

Fractional calculus - consisting of integrals and derivatives of arbitrary real and complex order - was first suggested in 1695 in correspondence between Leibniz and L'Hospital, though real-world applications have only begun to emerge intensely over the past few decades.

The first application of a fractional derivative (of order $1/2$) was done by Abel in 1823 [1], in relation to the tautochrone problem - find the curve shape that will have an object without friction in uniform gravity reach the lowest point at the same time, no matter the starting height. Though the tautochrone problem had been first presented in the 17th century, Abel was the first to find an analytical solution via fractional calculus.

Fractional derivatives are nonlocal in nature - they do not consider only local characteristics of dynamics, but instead take into account the global evolution of the entire system. For certain problems, this allows for more accurate models of real-world behavior than standard derivatives.

One simple example of this is the relationship between stress $\sigma(t)$ and strain $\epsilon(t)$ in a material under external forces. Both Newton's law for viscous liquid and Hooke's law for an elastic solid can be written as

$$\sigma(t) = \nu \frac{d^\alpha}{dt^\alpha} \epsilon(t)$$

where $\alpha = 1$ for Newton's law and $\alpha = 0$ for Hooke's. However, there exist materials that exhibit behavior somewhere in between (viscoelasticity), so it is useful to define the operator for $0 < \alpha < 1$.

One major benefit of using fractional derivatives is the so-called "memory effect." [8] Classic models of autonomous ODEs have no memory, as their solution does not depend on the previous instant. Given an initial value, the solution is uniquely determined for every point of the domain.

This makes fractional derivatives an attractive option for Stefan problems, since the unknown of the free boundary is dependent on all previous time steps.

Fractional calculus has been widely used in the modeling of evolutionary systems with memory effect on dynamics - physics, chemistry, biology, etc. For epidemiology, *hysteresis* effects can be incorporated into models. Hysteresis is a type of memory effect where the current state of the system depends on both current and past conditions.

In this chapter, we will give a general overview of a few basic fractional operators. We will then explore some important properties, motivating our choice of fractional operators for Stefan problems.

3.1 Fractional Derivatives: Overview

3.1.1 Preliminary Definitions

To develop the basics of fractional derivatives used in our work, we must first define a few basic functions that will prove useful.

The Gamma function $\Gamma(Z)$, a generalization of the factorial function, is defined for complex z where Re $z > 0$ as

$$\Gamma(z) = \int_0^\infty t^{z-1} e^{-t} dt.$$

The function is extended to the entire complex plane (with the exception of the simple poles on $\mathbb{Z}_{\leq 0}$). Useful properties include $\Gamma(1) = \Gamma(2) = 1$ and $\Gamma(z+1) = z\Gamma(z)$.

3.1.2 The Riemann-Liouville Fractional Integral

The first well-defined fractional operator is the Riemann-Liouville integral, an expansion of Cauchy's formula for repeated integration. There are various notations and definitions - we will begin with the classical definition, refining it further as we progress.

Definition 3.1.1. *Suppose that Re $\alpha > 0$ and $t > a$, where $a, t \in \mathbb{R}$. Then the Riemann-Liouville fractional integral of order α is*[1]

$$J^{\alpha} f(t) := \frac{1}{\Gamma(\alpha)} \int_a^t f(\tau)(t-\tau)^{\alpha-1} d\tau \tag{3.1}$$

Provided the function f is locally integrable and Re $\alpha > 0$, the Riemann-Liouville integral is well-defined. By convention, we have that $J^0 f(t) := f(t)$. A few essential properties are also immediately apparent:

$$\frac{d}{dt} J^{\alpha+1} f(t) = J^{\alpha} f(t) \tag{3.2}$$

$$J^{\alpha}(J^{\beta} f) = J^{\alpha+\beta} f \tag{3.3}$$

These properties are consistent with necessary properties for fractional differentiation. Additionally, the Riemann-Liouville integral defines a linear operator on $L^1(a, b)$. In fact, using Hölder's inequality, we find that if $f \in L^p(a, b)$, then $J^{\alpha} f \in L^p(a, b)$, and it can be shown that $J^{\alpha} : L^p(a, b) \to L^p(a, b)$ is a bounded linear operator.

3.1.3 The Riemann-Liouville Fractional Differential Operator

A natural consequence of the Riemann-Liouville integral is an accompanying differential operator. Again, there are varying definitions - here, we will adhere to those given by Gorenflo and Mainardi [11].

[1] Other common notations include I^{α} and ${}_a D_t^{-\alpha}$.

Definition 3.1.2. *Suppose that Re* $\alpha > 0$, $t > a$, *and* $t, a \in \mathbb{R}$. *Then*

$$D^{\alpha} f(t) := \begin{cases} \frac{1}{\Gamma(n-\alpha)} \frac{d^n}{dt^n} \int_a^t \frac{f(\tau)}{(t-\tau)^{\alpha+1-n}} d\tau, & n-1 < \alpha < n \in \mathbb{N} \\ \frac{d^n}{dt^n} f(t), & \alpha = n \in \mathbb{N} \end{cases} \tag{3.4}$$

The Riemann-Liouville derivative is the left inverse operator of the integral - that is,

$$D^{\alpha} J^{\alpha} f(t) = f(t)$$

and as with the integral, we conventionally define $D^0 f(t) := f(t)$.

3.1.4 The Caputo Fractional Differential Operator

In a paper in 1967 [6], Michele Caputo introduced an alternative fractional derivative, known as the Caputo derivative. Using the same constraints as the Riemann-Liouville derivative, we have the following definition.

Definition 3.1.3. *Suppose that* $t > a$, *Re* $\alpha > 0$, *and* $t, a \in \mathbb{R}$. *Then the Caputo fraction derivative is defined as*

$$D_*^{\alpha} f(t) := \begin{cases} \frac{1}{\Gamma(n-\alpha)} \int_a^t \frac{f^{(n)}(\tau)}{(t-\tau)^{\alpha+1-n}} d\tau, & n-1 < \alpha < n \in \mathbb{N} \\ \frac{d^n}{dt^n} f(t), & \alpha = n \in \mathbb{N} \end{cases} \tag{3.5}$$

Though the Riemann-Liouville and Caputo fractional derivatives appear to be similar, there are crucial differences. To show this, let us compare two different initial value problems (IVP).

$$\begin{gathered} D^{\alpha} y(t) - \lambda y(t) = 0 \\ \left[D^{\alpha-k-1} y(t) \right]_{t=0} = b_k \\ t > 0, \quad n-1 < \alpha < n, \quad k = 0, ..., n-1 \end{gathered} \tag{3.6}$$

$$
\begin{aligned}
D_*^{\alpha} y(t) - \lambda y(t) &= 0 \\
y^{(k)}(0) &= b_k \qquad (3.7) \\
t > 0, \quad n-1 < \alpha < n, \quad k &= 0, ..., n-1
\end{aligned}
$$

For the Riemann-Liouville IVP in (3.6), the fractional derivative is required as a part of the initial conditions. While this doesn't prevent the problem from being solved analytically, any physical interpretation of the condition is functionally useless.

However, for the Caputo IVP in (3.7), the initial conditions use integer order derivatives, with clear physical interpretations (e.g., $y(a)$ is position, $y'(a)$ is initial velocity, etc.). Note that this does require the existence of the k-th derivative of the function, but this is typically the case in applications.

3.2 Properties of the Caputo Fractional Derivative

In this section, we will prove some essential properties of the Caputo fractional derivative, alongside some comparisons to other fractional operators. More in depth analysis can be found in [14].

In general, when we refer to a function $f(t)$, we will be assuming that $f(t)$ is continuous, integrable for every finite interval $(0, x)$ for $x \in \mathbb{R}$, and

$$\lim_{t \to 0} t^r f(t) = \gamma \neq 0 \qquad (3.8)$$

for some constant γ, meaning that the function may have an integrable singularity of order $r < 1$ when $t = 0$. This will allow for our fractional operators from (3.1.1) and (3.1.2) to remain well-defined. To satisfy (3.1.3), we will also assume that the n-th derivative of $f(t)$ is integrable as well.

Note that from this point on, we will assume that for $n \in \mathbb{N}$,

$$D^n f(t) = \frac{d^n}{dt^n} f(t)$$

First, we can relate the Caputo fractional derivative to the Riemann-Liouville fractional integral.

Lemma 3.2.1. *Suppose $n-1 < \alpha < n \in \mathbb{N}$, and $\alpha \in \mathbb{R}$. Then it is true that*

$$D_*^\alpha f(t) = J^{n-\alpha} D^n f(t)$$
$$D^\alpha f(t) = D^n J^{n-\alpha} f(t)$$

In essence, this means that the Caputo fractional derivative is equivalent to $n-\alpha$ fold integration after nth integer order differentiation, whereas the Riemann-Liouville fractional derivative is the same but in reverse order.

Lemma 3.2.2. *Suppose that $n-1 < \alpha < n$, $n \in \mathbb{N}$, $\alpha \in \mathbb{R}$, and $f(t)$ such that $D_*^\alpha f(t)$ exists. Then*

$$\lim_{\alpha \to n} D_*^\alpha f(t) = f^{(n)}(t) \tag{3.9}$$
$$\lim_{\alpha \to n-1} D_*^\alpha f(t) = f^{(n-1)}(t) - f^{(n-1)}(0) \tag{3.10}$$

Proof. To prove both limits, we will use integration by parts.

$$\begin{aligned} D_*^\alpha f(t) &= \frac{1}{\Gamma(n-\alpha)} \int_0^t \frac{f^{(n)}(\tau)}{(t-\tau)^{\alpha+1-n}} d\tau \\ &= \frac{1}{\Gamma(n-\alpha)} \left(-f^{(n)}(\tau) \left. \frac{(t-\tau)^{(n-\alpha)}}{n-\alpha} \right|_{\tau=0}^t - \int_0^t -f^{(n+1)}(\tau) \frac{(t-\tau)^{n-\alpha}}{n-\alpha} d\tau \right) \\ &= \frac{1}{\Gamma(n-\alpha+1)} \left(f^{(n)}(0) t^{n-\alpha} + \int_0^t f^{(n+1)}(\tau)(t-\tau)^{n-\alpha} d\tau \right) \end{aligned}$$

Now it's simply a matter of applying each limit.

$$\begin{aligned}\lim_{\alpha\to n} D_*^\alpha f(t) &= \frac{1}{\Gamma(1)}\left(f^{(n)}(0) + f^{(n)}(\tau)\right)\Big|_{\tau=0}^{t} \\ &= f^{(n)}(t)\end{aligned}$$

$$\begin{aligned}\lim_{\alpha\to n-1} D_*^\alpha f(t) &= \frac{1}{\Gamma(2)}\left(f^{(n)}(0)t + f^{(n)}(\tau)(t-\tau)\right)\Big|_{\tau=0}^{t} - \int_0^t -f^{(n)}(\tau)d\tau \\ &= f^{(n-1)}(\tau)\Big|_{\tau=0}^{t} \\ &= f^{(n-1)}(t) - f^{(n-1)}(0)\end{aligned}$$

□

For the Riemann-Liouville derivative, the limits are similar.

$$\lim_{\alpha\to n} D^\alpha f(t) = f^{(n)}(t)$$
$$\lim_{\alpha\to n-1} D^\alpha f(t) = f^{(n-1)}(t)$$

Both the Riemann-Liouville and Caputo derivatives are also linear operators. The proof for both derivatives follows immediately from the definitions in (3.1.2) and (3.1.3).

Lemma 3.2.3. *Suppose $n-1 < \alpha < n$ for $n \in \mathbb{N}$, $\alpha, \lambda \in \mathbb{C}$, and functions $f(t), g(t)$ are such that D_*^α and D^α exist. Then*

$$D_*^\alpha(\lambda f(t) + g(t)) = \lambda D_*^\alpha f(t) + D_*^\alpha g(t)$$
$$D^\alpha(\lambda f(t) + g(t)) = \lambda D^\alpha f(t) + D^\alpha g(t)$$

Up until this point, we have been focused on the general order α where $n-1 < \alpha < n \in \mathbb{N}$. However, it is sufficient to find the Caputo derivative of order $\beta = \alpha - (n-1)$ - though both the Riemann-Liouville and Caputo derivatives are non-commutative, they do have similar properties that allow them to be reduced to the fractional portion of the derivative.

Lemma 3.2.4. *Suppose that $n-1 < \alpha < n$, and $m, n \in \mathbb{N}$, with $\alpha \in \mathbb{R}$. Then, in general,*

$$D_*^\alpha D^m f(t) = D_*^{\alpha+m} f(t) \neq D^m D_*^\alpha f(t)$$
$$D^m D^\alpha f(t) = D^{\alpha+m} f(t) \neq D^\alpha D^m f(t)$$

Corollary 3.2.5. *Suppose that $n-1 < \alpha < n \in \mathbb{N}$, and $\beta = \alpha - (n-1)$ so that $0 < \beta < 1$ for $\alpha, \beta \in \mathbb{R}$. Then from 3.2.4, it immediately follows that*

$$D_*^\alpha f(t) = D_*^\beta D^{n-1} f(t)$$

One of the primary differences between the Riemann-Liouville and Caputo derivatives is the treatment of the constant function. In real world applications, it is useful to have the derivative (fractional or otherwise) of a constant equal to zero. This does *not* hold for the Riemann-Liouville derivative, but it does for Caputo.

Lemma 3.2.6. *For the Caputo fraction derivative, if $c =$constant, then*

$$D_*^\alpha c = 0$$

Proof. For $0 < n-1 < \alpha < n \in \mathbb{N}$, we have that $n \geq 1$, so applying the definition in 3.1.3 and using the fact that integer-order derivatives of constants are 0,

$$D_*^\alpha = \frac{1}{\Gamma(n-\alpha)} \int_a^t \frac{c^{(n)}}{(t-\tau)^{\alpha+1-n}} d\tau = 0$$

□

3.3 The Caputo Laplace Transform

We have thus far established basic properties of fractional operators, and we have also highlighted the motivations for using the Caputo fractional derivative in real world applications. To apply the Caputo derivative to differential equations, it is useful to find the Laplace transform, particularly for initial value problems on a semi-infinite domain.

We will begin with the general definition.

Definition 3.3.1. *If the function below exists for $s \in \mathbb{C}$, it is called the Laplace transform of $f(t)$.*

$$F(s) := L\{f(t); s\} := \int_0^\infty e^{-st} f(t) dt$$

For the Laplace transform to exist, the following conditions are sufficient, from [12]

1. $f(t)$ must be piecewise smooth over all finite intervals in $[0, \infty)$
2. $f(t)$ must be of exponential order α, such that there exist constants $M, T > 0$ where $|f(t)| \leq Me^{\alpha t}$ for all $t > T$

We of course wish to find the Laplace transform of the Caputo fractional derivative. To do so, we will first need to establish Laplace transforms of a few basic operators. The proof for this lemma can be found in [19].

Lemma 3.3.2. *Suppose that $p > 0$, and that $F(s)$ is the Laplace transform of the function $f(t)$. Then the following hold.*

1. *The Laplace transform of the fractional integral of order α stated in 3.1.1 is given by*

$$L\{J^\alpha f(t); s\} = s^{-\alpha} F(s)$$

2. *For $n-1 < \alpha < n$, the Laplace transform of the Riemann-Liouville fractional derivative stated in 3.1.2 is given by*

$$\begin{aligned} L\{D^\alpha f(t); s\} &= s^\alpha F(s) - \sum_{k=0}^{n-1} s^k \left[D^{\alpha-k-1} f(t)\right]_{t=0} \\ &= s^\alpha F(s) - \sum_{k=0}^{n-1} s^{n-k-1} \left[D^k J^{n-\alpha} f(t)\right]_{t=0} \end{aligned}$$

We can use these two statements to define and prove the Laplace transform of the Caputo fractional derivative.

Theorem 3.3.3. *Suppose the $p > 0$, and that $F(s)$ is the Laplace transform of the function $f(t)$. Then the Laplace transform of the Caputo fractional derivative for $n-1 < \alpha < n$ is given by*

$$L\{D_*^\alpha f(t); s\} = s^\alpha F(s) - \sum_{k=0}^{n-1} s^{\alpha-k-1} f^{(k)}(0)$$

Proof. To prove that 3.3.3 is valid, we will use our preliminary definitions from earlier. First, let us consider the Caputo derivative in relation to the fractional integral 3.2.1, and let $g(t) := D^n f(t)$.

$$D_*^\alpha f(t) = J^{n-\alpha} D^n f(t) \tag{3.11}$$

$$= J^{n-\alpha} g(t) \tag{3.12}$$

Then, we can use the Laplace of the fractional integral in 3.3.2 of order $n-\alpha$ to rewrite as

$$L\{D_*^\alpha f(t); s\} L\{J^{n-\alpha} g(t); s\} = s^{-(n-\alpha)} G(s)$$

where $G(s) = L\{g(t); s\}$. Using a basic property of the Laplace transform, we can expressed $G(s)$ as

$$G(s) = s^n F(s) - \sum_{k=0}^{n-1} s^{n-k-1} f^{(k)}(0) \tag{3.13}$$

Then it is simply a matter of substitution to obtain our result

$$L\{D_*^\alpha f(t); s\} = s^{-(n-\alpha)} \left(s^n F(s) - \sum_{k=0}^{n-1} s^{n-k-1} f^{(k)}(0) \right) = s^\alpha F(s) - \sum_{k=0}^{n-1} s^{\alpha-k-1} f^{(k)}(0)$$

so the theorem is proved. □

Here, we will pause to make a few comments about our work in fractional operators thus far. First, we have established that the Caputo fractional differential operator is better for

physical applications than the Riemann-Liouville derivative, especially due to the derivative of a constant function remaining zero.

For the Laplace transform, we can see some additional benefits. First, for the Riemann-Liouville Laplace transform in 3.3.2, we require initial values of the fractional integral $J^{n-\alpha}$ as well as integer derivatives of order $k = 1, ..., n-1$. However, for the Caputo Laplace transform, we need only the initial values of the function $f(t)$ (as well as the integer derivatives).

The Laplace transform of the Caputo derivative is also a generalization of the Laplace transform of the integer-order derivative. However, this is not true of the Riemann-Liouville operator.

3.3.1 Advantages and Disadvantages

As we have stated, the Caputo fractional derivative allows us to use traditional initial and boundary conditions, in addition to having the derivative of a constant be zero. This makes the Caputo derivative the best fractional operator to use for real-world problems.

However, the Caputo derivative is not perfect. In order to compute the Caputo derivative, we must first calculate its standard derivative. In addition, Caputo derivatives are defined only for differentiable functions. Functions with no first-order derivative may still have Riemann-Liouville derivatives, allowing for more general use and flexibility. Further discussion regarding the advantages and disadvantages of various fractional operators can be found in [11], [2], and [14].

3.4 Conclusions

In this chapter, we have established preliminary definitions of fractional operators, and explored two prominent fractional differential operators with various comparisons of properties. It is now clear that the Caputo derivative is the most useful fractional derivative for real

world applications - some examples, including the fractional damped harmonic oscillator, can be found from Podlubny [19] and Debnath [7]. Additionally, the Caputo fractional derivative has been implemented to calculate approximate solutions of initial boundary value problems by Gordievskikh D.M. and Davydov P.N. [10].

The benefits of using fractional operators are apparent when there are "in-between" states - such as the example of viscoelasticity stated at the beginning of this chapter, when integer-order derivatives are not sufficient to properly model physical states. Our goal is to apply the Caputo fractional differential operator to the one-phase Stefan problem in both one and two dimensions, developing a flexible numerical model that can be adjusted for physical parameters as needed.

CHAPTER FOUR

THE STEFAN CAPUTO MODEL

Now that we have established both the Stefan problem and the Caputo fractional derivative, we will build our model.

As we determined in Chapter 2, the classical solution to the one-phase, one-dimensional Stefan problem predicts the location of the free boundary proportional to $\sqrt{t}$. But for diffusion processes and materials that follow from non-classical physical assumptions (with phase transitions nonlocal in time), we can use the Caputo derivative to take advantage of the memory effect.

Applications of fractional operators to Stefan problems has been only recently begun to be explored for numerical approaches. Results from Roscani [21] explore fractional approaches to Stefan-like problems linked to anomalous diffusion. Using the fractional Caputo derivative for the one-dimensional, one-phase Stefan problem has been proposed using the front-fixing method to the subdiffusion case by [4]. Our model aims to have a flexible numerical approach, using the finite difference scheme with the SOR method in both one and two dimensions.

4.1 The One-Dimensional Model

We will begin with the one-phase one-dimensional model, under the same assumptions stated in Chapter 2 - negligible volume change, with a constant temperature in the solid region. Substituting the Caputo fractional derivative into the model from 2.8, we obtain the following problem.

$$D_t^\alpha u(x,t) = \frac{\partial^2 u}{\partial x^2} \qquad 0 < x < s(t), t > 0 \tag{4.1}$$

$$LD_t^\alpha s(t) = -\frac{\partial u}{\partial x}\Big|_{x=s(t)^-} \qquad t > 0 \tag{4.2}$$

$$u(0,t) = T_1 > 0 \qquad t > 0 \tag{4.3}$$

$$u(x,t)\Big|_{x=s(t)^-} = 0 \qquad t > 0 \tag{4.4}$$

$$s(0) = 0 \tag{4.5}$$

Note that here, we represent the Caputo fractional derivative with D_t^α (rather than the aforementioned D_*^α), using the t to denote the associated variable.

To account for the new derivative and the latent heat, we will also need to track the enthalpy of the system. As discussed earlier, enthalpy is a state function of a thermodynamic system, the sum of its internal energy and the product of pressure and volume. In this case, we track enthalpy as the sum of the latent heat and the temperature.

From here on, we are replacing temperature u with a scaled temperature $\tilde{u}$, where $\tilde{u} = c_p u$, and c_p is the thermal heat capacity at constant pressure, so that $c_p\tilde{u}$ has the same units as intensive enthalpy. Using the fact that $dh = Tds + dp\rho$, where s is the intensive entropy, we can have $h = c_p T$ where $c_p = \frac{\partial h}{\partial T}\big|_p$.

For the remainder of this document, we will replace $\tilde{u}$ with u and h with H, for ease of notation.

$$H(x,t) = \begin{cases} u + L & \text{if } u > 0 \\ [0, L] & \text{if } u = 0 \end{cases} \tag{4.6}$$

Since this enthalpy definition (4.6) has multiple outputs for a single input (one-to-many), we will clearly need to adjust this definition numerically so that there is a function.

The initial state of the substance is solid, with phase transition temp $T_0 = u_0 = 0$, and $H(x,t) = 0$.

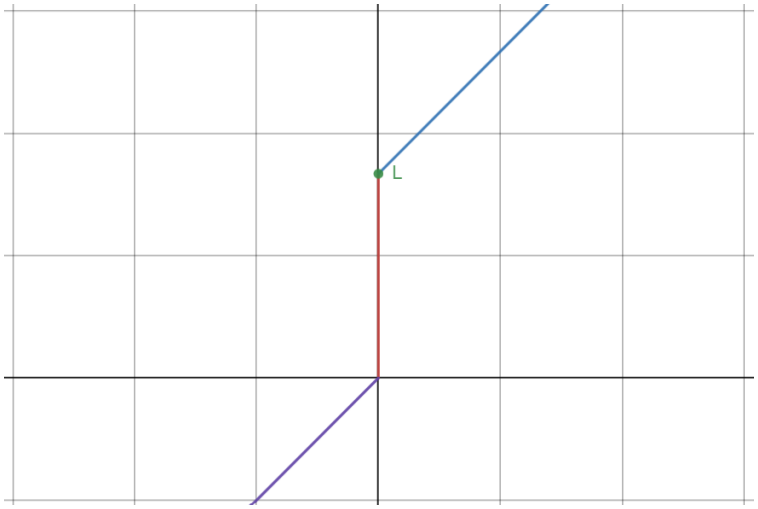

Figure 4.1 Graph of enthalpy function $H(u)$

4.1.1 Finite Difference Scheme

We will then approximate the problem using a finite-difference scheme on a uniform mesh. A finite difference method is technique for solving differential equations by approximating the derivative[18]. There are many ways to approximate, including explicit methods using a forward difference for time and a central difference for space, which is numerically stable and convergent as long as the value $r = \frac{\tau}{h^2} \leq 0.5$. [15] [20]

In the figure below, the node (i, j) represents the space i and time j. The memory effect of the fractional derivative will use all previous time steps to calculate the finite difference discretization, while linked space nodes contribute heat. [5]

The L_1 approximation of the Caputo fractional derivative at a fixed time k is constructed by approximating the function $v(t)$ with the continuous and piecewise linear function.

$$
\begin{aligned}
D_t^\alpha v(t_k) \approx \partial_t^\alpha \overline{v^k} &= \frac{1}{\Gamma(1-\alpha)} \sum_{j=1}^{k} \frac{v^j - v^{j-1}}{\tau} \int_{s=t_{j-1}}^{t_j} (t_k - s)^{-\alpha} ds \\
&= d_1 v^k + \sum_{j=1}^{k-1} (d_{j+1} - d_j) v^{k-j} - d_k v^0
\end{aligned}
$$

Here, $\overline{v^k} = (v^0, v^1, ..., v^k)$, and

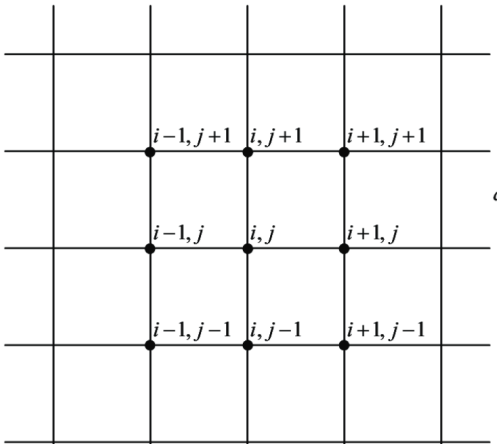

Figure 4.2 Uniform mesh grid

$$d_j = \frac{j^{1-\alpha} - (j-1)^{1-\alpha}}{\tau^\alpha \Gamma(2-\alpha)}$$

Next, we approximate the Caputo fractional derivative using the finite difference discretization. Note that here, we will use subscript i for space and k time.

$$d_1 H_i^k + \sum_{j=1}^{k-1} (d_{j-1} - d_j) H_i^j + \frac{1}{h^2}(2u_i^k - u_{i-1}^k - u_{i+1}^k) = 0 \tag{4.7}$$

$$d_j = \frac{j^{1-\alpha} - (j-1)^{1-\alpha}}{\tau^\alpha \Gamma(2-\alpha)} \tag{4.8}$$

$$d_1 = \frac{1}{\tau^\alpha \Gamma(2-\alpha)} \tag{4.9}$$

Now, let us fix time level $k \geq 1$ to give us the following scheme.

$$d_1 H_1^k + \frac{1}{h^2}(2u_i^k - u_{i-1}^k - u_{i+1}^k) = -\sum_{j=1}^{k-1} (d_{j+1} - d_j) H_i^{k-j} \tag{4.10}$$

Fix time level k and introduce notation $u^k = u$, $H^k = \xi$, and let F replace the right side of equation 4.10.

4.1.2 SOR Method

We choose to use the successive over-relaxation method to solve. The SOR method[25], a variant of Gauss-Seidel, is useful for converging iterative processes.[24] Then we have that $0 < \omega < 2$ is our SOR parameter, also known as the relaxation factor.

The steps are outlined below.

1. Choose initial guess u^0 and ξ^0, and iterate to obtain u_i^n (where n is the iteration, not the time step) from

$$\frac{2}{\omega h^2} u_i^n + d_1 \xi_i = F_i + \frac{2}{h^2}(\frac{1}{\omega} - 1) u_i^{n-1} + \frac{1}{h^2} u_{i-1}^n + \frac{1}{h^2} u_{i+1}^{n-1}$$

2. Denote the right hand side by G_i, we have

$$\frac{2}{\omega h^2} u_i + d_1 \xi_i = G_i$$

3. Update the space node, depending on the outcome.

   (a) If we have that $G_i - d_1 L > 0$, then update the space node

$$u_i = \frac{G_i - d_1 L}{\frac{2}{\omega h^2} + d_1}$$

   (b) Otherwise, let $u_i = 0$

As this process continues, we are updating each space node for the fixed time k, then taking one time step and repeating. The finite difference discretization takes in the previous solutions - the "memory effect" from the Caputo fractional derivative - and pushes the free boundary $s(t)$ further down the slab. The block diagram for the algorithm is depicted in Appendix A.

4.2 The Two-Dimensional Model

The two-dimensional model is developed in a similar way. We begin with the statement of the problem, establishing the Caputo fractional derivatives for the heat equation in the liquid region as well as the Stefan condition.

For the two dimensional problem on the domain $\Omega = [0,1] \times [0,1]$, the enthalpy equation takes the form

$$D_t^\alpha H(x,t) - \delta u(x,t) = 0 \tag{4.11}$$

The uniform mesh presented for the one-dimensional problem will be similar for two dimensions. Written out explicitly, we obtain

$$y_{i,j} = d_1 \left(H_{i,j}^k + \sum_{s=1}^{k-1} \left((s+1)^{1-\alpha} - 2s^{1-\alpha} + (s-1)^{1-\alpha} \right) H_{i,j}^{k-s} - \left(k^{1-\alpha} - (k-1)^{1-\alpha} \right) H_{i,j} \right) + \frac{1}{h^2} \left(4u_{i,j}^k - u_{i+1,j}^k - u_{i-1,j}^k - u_{i,j+1}^k - u_{i,j-1}^k \right) = 0 \tag{4.12}$$

As with the one-dimensional problem, we will need to deal with the ambiguity of the enthalpy itself. The value of H at the phase change boundary is $[0, L]$, and the temperature is zero as well. Since the temperature is known, we can use that to solve for the enthalpy, transforming 4.12 into the following:

$$\frac{2\tau^\alpha \Gamma(2-\alpha) u_i^k}{\sigma h^2} + H_i^k = \sum_{j=1}^{k-1} \left(-(j+1)^{1-\alpha} + 2j^{1-\alpha} - (j-1)^{1-\alpha} \right) H_i^{k-j} - (k^{1-\alpha} - (k-1)^{1-\alpha}) H_i^0 + \frac{1}{h^2} \left(\tau^\alpha \Gamma(2-\alpha)(u_{i+1,j}^{k-1} + u_{i-1,j}^k + u_{i,j+1}^{k-1} + u_{i,j-1}^k) + \frac{1-\sigma}{\sigma} \overline{u_{i,j}^k} \right) \tag{4.13}$$

This equation 4.13 is checked to see if it falls into the range of $[0, L]$. The enthalpy function for two dimensions is

$$H_{i,j}^{k}(u) = \begin{cases} (4.13) & \text{if } (4.13) \leq L \\ u_{i,j}^{k} + L & \text{if } (4.13) > L \end{cases} \tag{4.14}$$

Now, at each time layer, we need to calculate the error as well for the SOR condition. To do so, we simply need to check the L_2 norm of 4.12:

$$\|y^k\|_{L_2} = \left(\sum_{1 \leq i,j \leq m} (y_{i,j}^{k})^2 \right)^{1/2} < \varepsilon \tag{4.15}$$

If this inequality holds, we will move to the next time step. Otherwise, we move to the $k+1$ iteration and recalculate the temperature and enthalpy values for each space node.

CHAPTER FIVE

RESULTS

5.1 One-Dimensional Model

For the initial basic model, we performed small-scale experiments with space and time divided into 100 intervals.

To begin, recall that the constants from the Stefan problem defined in Chapter 2 are assumed to be equal to one, since this model is not restricted to one particular type of material. For our model, we only wish to determine the temperature values and the movement of the phase boundary. Thus the essential parameters were the α value of the Caputo fractional derivative, the temperature of the heat source, and the latent heat value L.

5.1.1 Alpha Values

A natural avenue for exploration is to adjust the α value for the Caputo fractional derivative. First, from our results in Chapter 2, we know that for the one-phase and one-dimensional form, the movement of the phase boundary is proportional to $\sqrt{t}$ as $\alpha \to 1^{-}$. In figure (5.1), we can see that our model matches this similarity solution.

It's easier to see this with a direct comparison, using a log scale. In figure (5.2), we have graphed both the free boundary for $\alpha \to 1$, as well as the function $ln(y) = 0.5ln(t) + b$, with both axes on a logarithmic scale - it's clear that the slopes match, when shift the function up to match starting values.

For figure 5.1, the temperature at the heat source is $5°C$. The $x-$axis shows the time, divided into 100 equally spaced intervals, while the vertical $y-$axis shows the number of

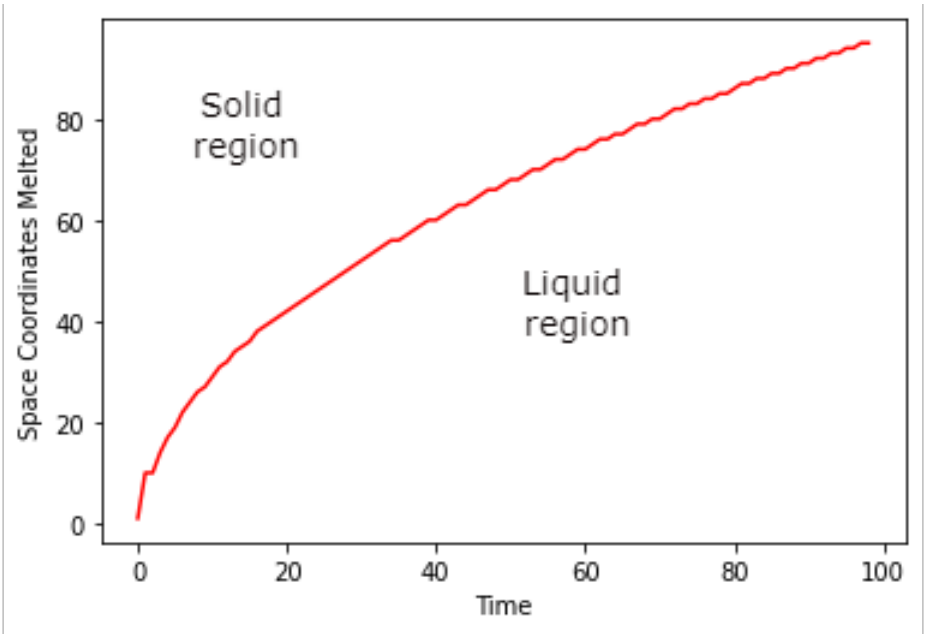

Figure 5.1 Graph for $\alpha \to 1$ showing the movement of the free boundary over time

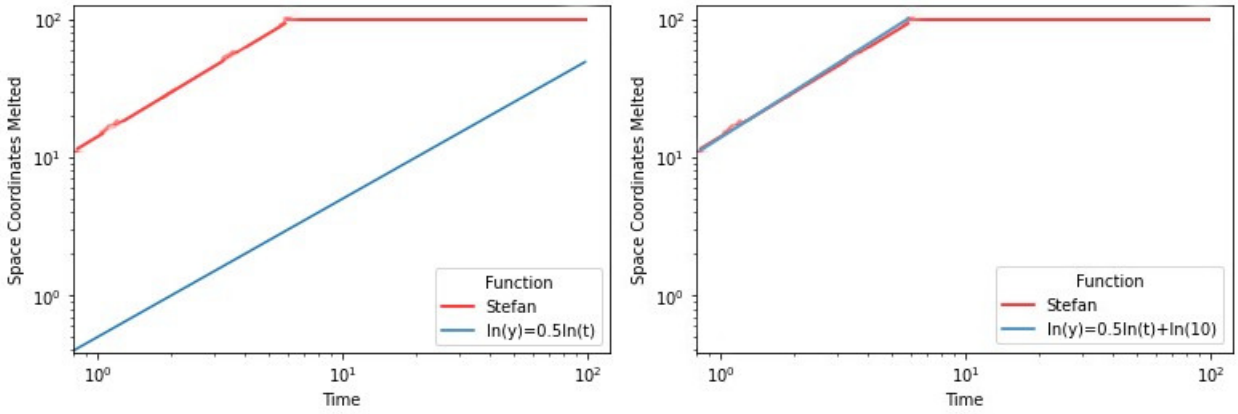

Figure 5.2 Comparison between the free boundary for $\alpha \to 1$ and $ln(y) = 0.5ln(t)+b$

space coordinates $x \in [1, 100]$ that have melted from solid to liquid.

Next, we wish to test various α values. We expect that as the value of α decreases, the phase boundary will move at a faster rate, as the fractional portion of the derivative increases the "memory effect."

For these tests, the heat source temperature is $10°C$, with 100 time steps.

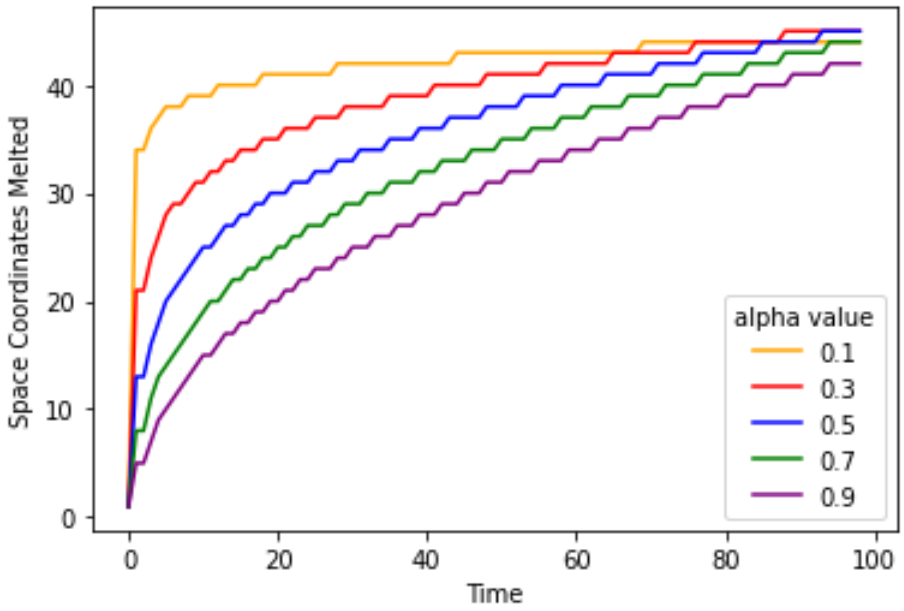

Figure 5.3 The movement of the phase boundary for varying alpha values

The results in figure 5.3 are just as expected. For $\alpha = 0.1$, we can see that the melting rate is significantly faster than, say, $\alpha = 0.9$.

5.1.2 Initial Temperatures

Next, we want to explore the movement of the phase boundary $s(t)$ for varying initial temperatures. Intuitively, it makes sense that a hotter heat source will cause the slab of ice to melt at a faster rate - conversely, a very low temp at the heat source may see very little of the slab melt in the same amount of time steps.

From figure 5.4, the higher heat source temperatures correspond to a faster melting rate - in fact, for heat source temperatures $20°C$ and $50°C$, the entire slab is melted during the process.

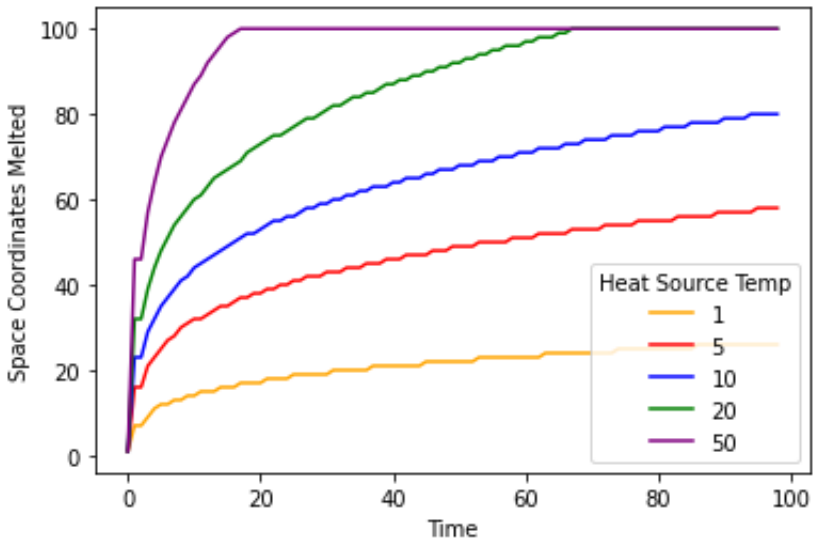

Figure 5.4 The movement of the phase boundary for varying heat source temperatures

5.1.3 Latent Heat

The last parameter to explore is the latent heat. Since latent heat is the energy needed to undergo the phase change, we expect that lower values of latent heat will cause the phase boundary to move faster than those with high values of latent heat.

As we can see in figure 5.5, the differences in latent heat do affect the movement of the phase boundary. Low latent heat values, such as 11.4 kJ/kg for mercury, correspond to faster melting times, as the material needs much less energy to change from solid to liquid.

In table (5.1) below, we can see a summary of the one-dimensional tests. The phase boundary location is out of 100 space nodes, showing the farther melted node, after 100 time steps.

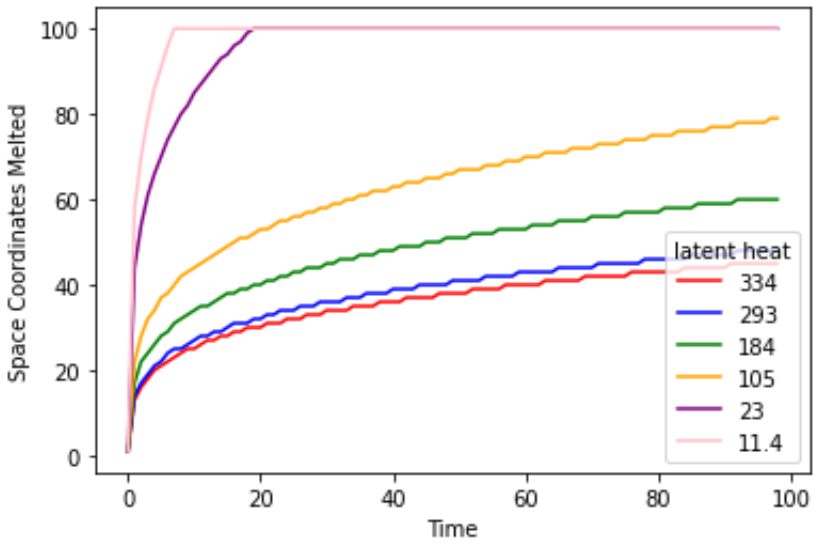

Figure 5.5 The movement of the phase boundary for various latent heat values.

Heat Source Temp	Alpha Value	Latent Heat	Phase Boundary Loc.
1	0.5	100	26
5	0.5	100	57
10	0.5	100	80
20	0.5	100	100
50	0.5	100	100
10	0.5	11.4	100
10	0.5	23	100
10	0.5	105	78
10	0.5	184	60
10	0.5	293	47
10	0.5	334	44

Table 5.1 Summary of parameter comparisons for the one-dimensional model.

5.2 Two-Dimensional Model

For our two dimensional model, we have more parameters to explore. While the temperature of the heat source clearly has an effect on the speed of the phase boundary, in two dimensions we can also shift the location of the heat source.

To reduce our computing time, the experiments run for the two-dimensional model were smaller, with 20x20 space nodes and 20 time nodes.

5.2.1 Alpha Values

Our first iteration was for $\alpha = 0.5$, with the latent heat of 334kJ/kg. We chose a uniform heat source temperature of $10°C$. Because we are now in two dimensions, the energy contributing to each space node is not only from the node directly before it, but from all nodes surrounding it.

This means that space nodes on the upper and lower boundaries of the region will have less contribution of energy, while nodes in the center of the region will have more. So we expect the phase boundary to be a curve protruding from the center.

As we can see in figure 5.6, this is in fact the case. The bottom left axis is time t, while the vertical plane is the temperature of the melted space nodes.

To better understand the 3D plots, we can take a slice at fixed time k. The heat map in figure 5.7 is the entire 2D space at time $k = 20$ - you can see that the curvature matches the vertical slice of the 3D plot.

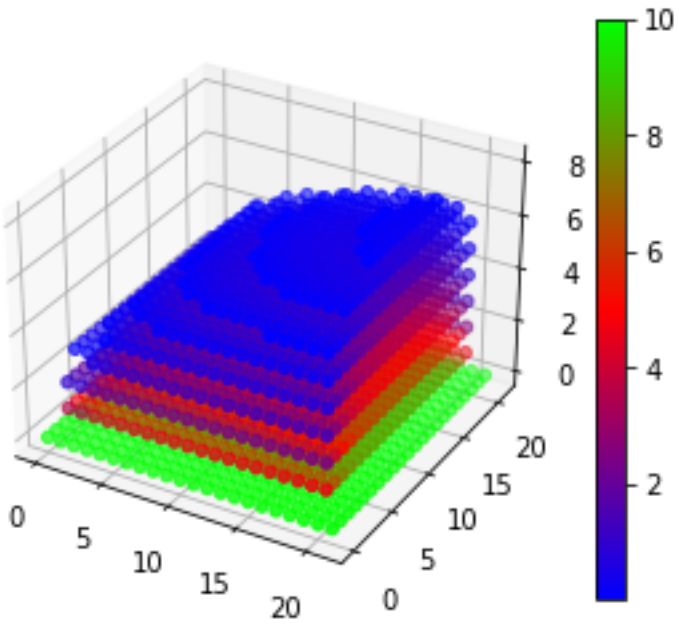

Figure 5.6 3D plot of the two-dimensional Stefan Caputo model for $\alpha = 0.5$

	0	1	2	3	4	5	6	7	8	9	10	11
0	10	0	0	0	0	0	0	0	0	0	0	0
1	10	4.69631	2.51174	1.42918	0.80347	0.401178	0.131302	0	0	0	0	0
2	10	6.45032	4.08563	2.55989	1.54443	0.843718	0.353425	0.0292667	0	0	0	0
3	10	7.20781	4.9958	3.34691	2.13494	1.24549	0.601572	0.169882	0	0	0	0
4	10	7.57879	5.52473	3.86969	2.57165	1.57188	0.820843	0.29149	0	0	0	0
5	10	7.77898	5.84045	4.21231	2.8823	1.82144	0.998993	0.392983	0	0	0	0
6	10	7.89454	6.03407	4.43647	3.0986	2.00607	1.1407	0.489065	0.0545156	0	0	0
7	10	7.96391	6.15469	4.58249	3.24624	2.13849	1.24886	0.571672	0.118295	0	0	0
8	10	8.00578	6.22921	4.67548	3.34346	2.22887	1.32562	0.632287	0.161555	0	0	0
9	10	8.02975	6.27247	4.73052	3.4023	2.28484	1.37415	0.670667	0.187012	0	0	0
10	10	8.04069	6.29237	4.75612	3.43001	2.31154	1.39752	0.689145	0.198987	0	0	0
11	10	8.04069	6.29237	4.75612	3.43001	2.31154	1.39752	0.689145	0.198987	0	0	0
12	10	8.02975	6.27247	4.73052	3.4023	2.28484	1.37415	0.670667	0.187012	0	0	0
13	10	8.00578	6.22921	4.67548	3.34346	2.22887	1.32562	0.632287	0.161555	0	0	0
14	10	7.96391	6.15469	4.58249	3.24624	2.13849	1.24886	0.571672	0.118295	0	0	0
15	10	7.89454	6.03407	4.43647	3.0986	2.00607	1.1407	0.489065	0.0545155	0	0	0
16	10	7.77898	5.84045	4.21231	2.8823	1.82144	0.998993	0.392983	0	0	0	0
17	10	7.57879	5.52473	3.86969	2.57165	1.57188	0.820843	0.29149	0	0	0	0
18	10	7.20781	4.9958	3.34691	2.13494	1.2455	0.601572	0.169881	0	0	0	0
19	10	6.45032	4.08563	2.55989	1.54443	0.843719	0.353425	0.0292665	0	0	0	0
20	10	4.69631	2.51174	1.42918	0.80347	0.401178	0.131302	0	0	0	0	0
21	10	0	0	0	0	0	0	0	0	0	0	0

Figure 5.7 Heat map of the 2D region at fixed time $k = 20$

Next, we can test various alpha values of the fractional operator. We expect that smaller values of α will result in more of the plane melting in the same amount of time, since lower values increase the "memory effect" of the Caputo derivative.

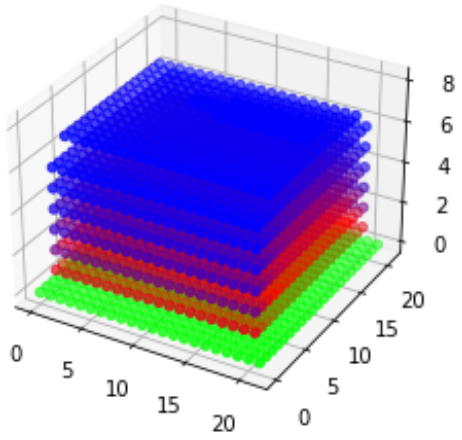

(a) $\alpha = 0.01$

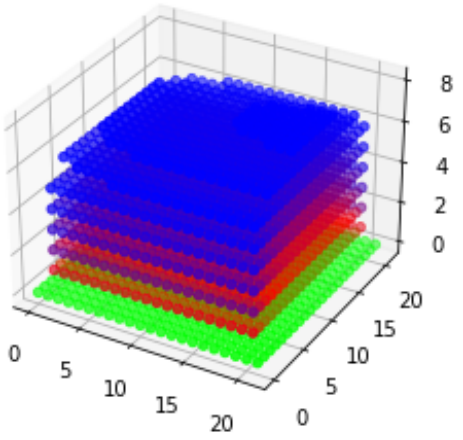

(b) $\alpha = 0.1$

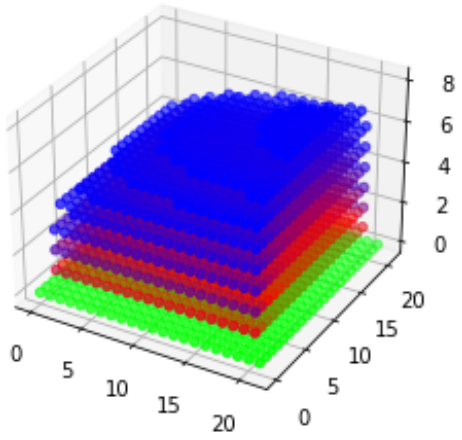

(c) $\alpha = 0.3$

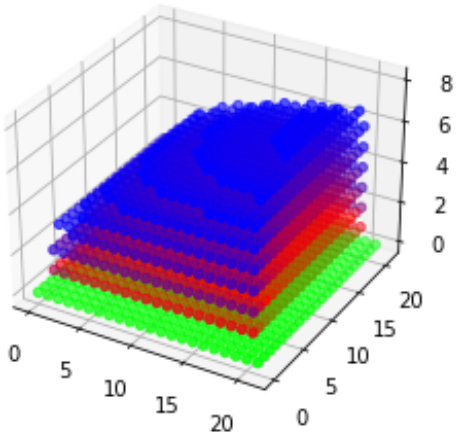

(d) $\alpha = 0.5$

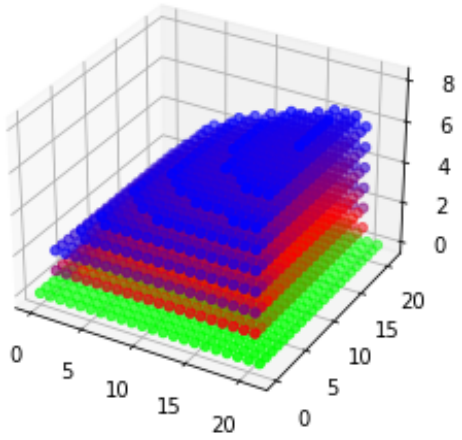

(e) $\alpha = 0.7$

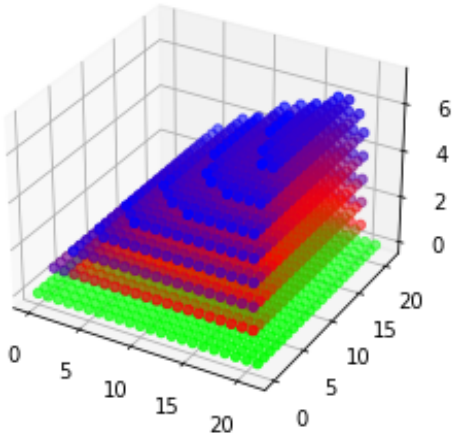

(f) $\alpha \to 1$

Figure 5.8 3D plots of the two-dimensional model for varying α values

5.2.2 Latent Heat

As with the one-dimensional model, we can adjust the various parameters to ensure that our model is working as expected. For the latent heat value L, we can test that same materials we did before, using 20 time nodes and 20x20 space nodes.

As expected, in figure 5.9 we can see that lowering the latent heat values causes more of the plane to melt during the allotted time.

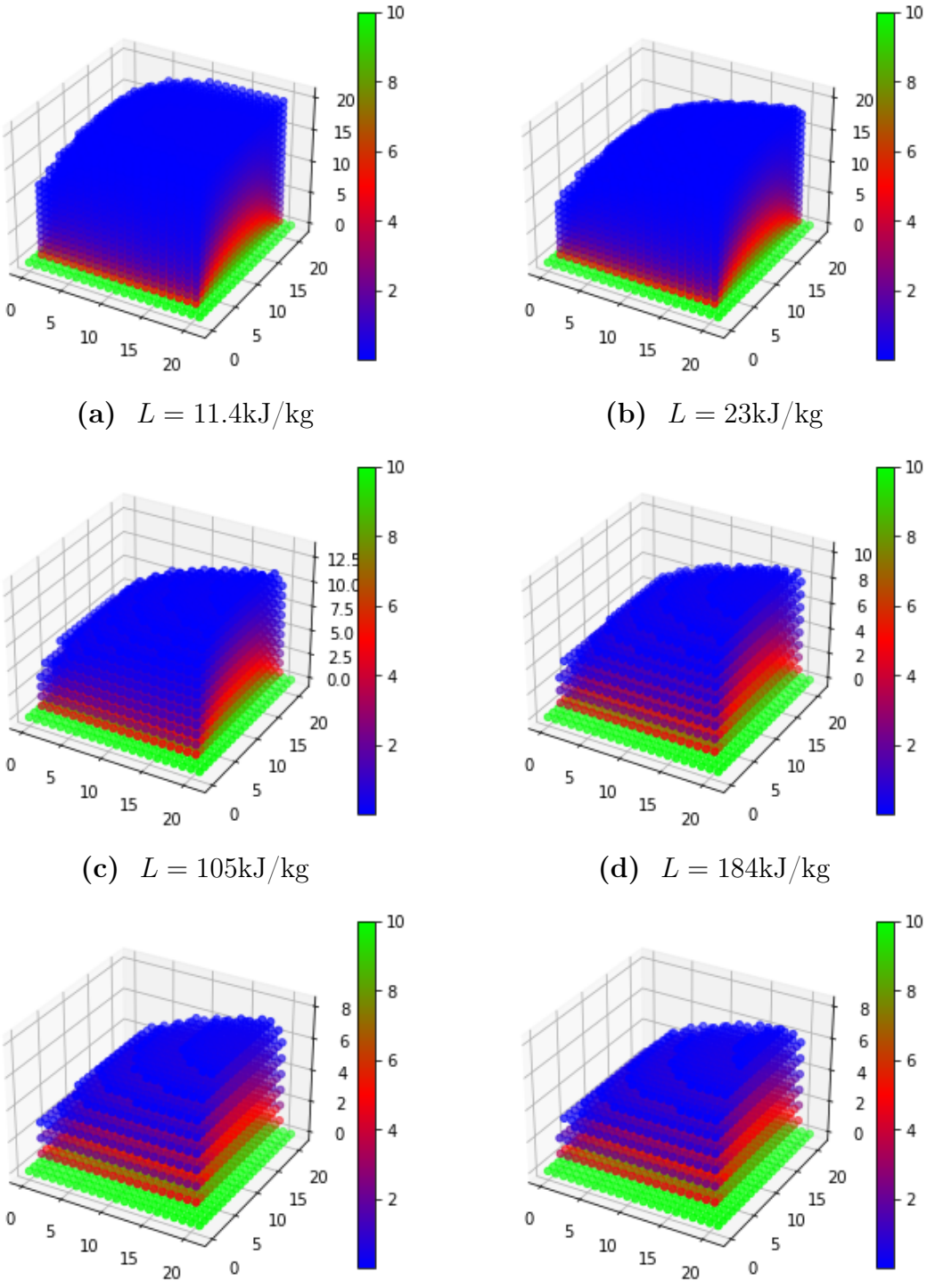

(a) $L = 11.4\text{kJ/kg}$ **(b)** $L = 23\text{kJ/kg}$

(c) $L = 105\text{kJ/kg}$ **(d)** $L = 184\text{kJ/kg}$

(e) $L = 293\text{kJ/kg}$ **(f)** $L = 334$

Figure 5.9 3D plots of the two-dimensional model for varying latent heat values

5.2.3 Heat Source Variation

In two dimensions, our heat source can be represented as a rod with length l on one boundary of the two-dimensional space. With the entire rod at a constant temperature, we can see that higher initial temperatures result in faster melting rates.

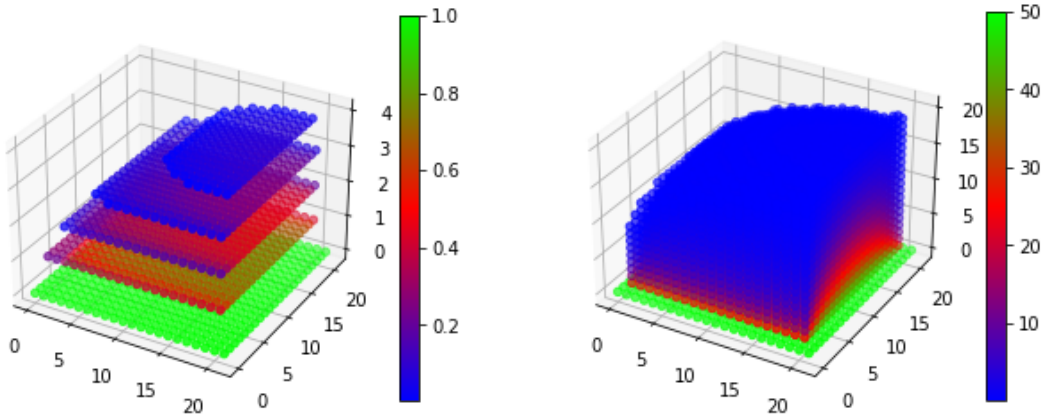

(a) $1°C$

(b) $50°C$

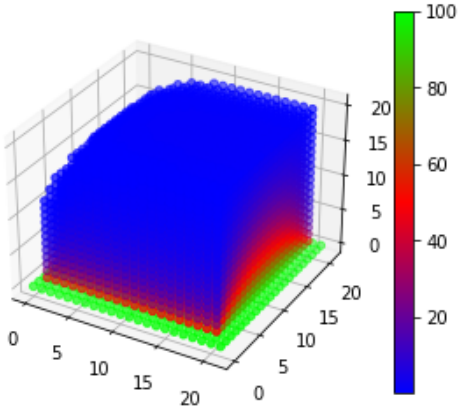

(c) $100°C$

Figure 5.10 3D plots of the two-dimensional model for varying heat source temperatures

However, we can also make the heat source more concentrated in different regions of the rod.

Rather than keeping the heat source as a uniform temperature, we can instead regard the source as a heat gradient, with a central high temperature tapering outward. When applied

to our model, we can see that the phase boundary reflects the concentrated higher heat and dissipates outward.

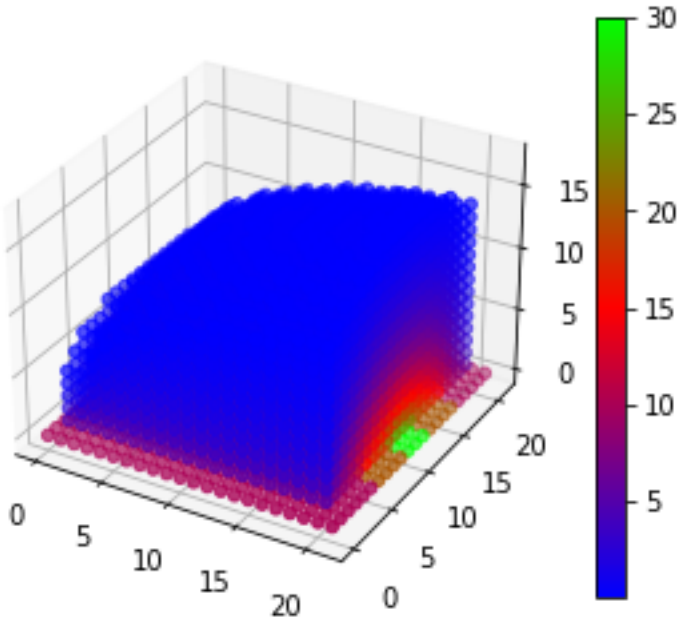

Figure 5.11 3D plot showing the model with a central heat source radiating outward

In figure 5.11, the heat source ranges from $10°C$ to $30°C$.

Similarly, we can concentrate the heat source in the center and keep the surrounding nodes at $0°C$, or concentrate on one of the edges.

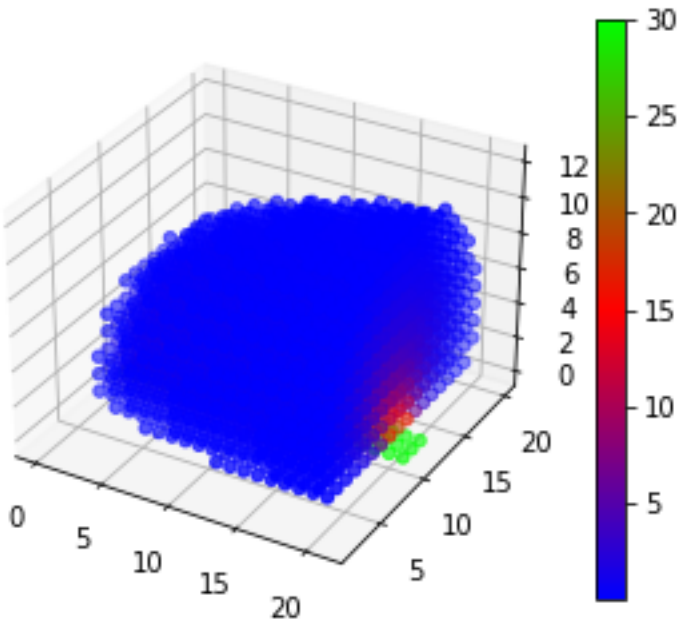

Figure 5.12 3D plot showing the model with a concentrated central heat source

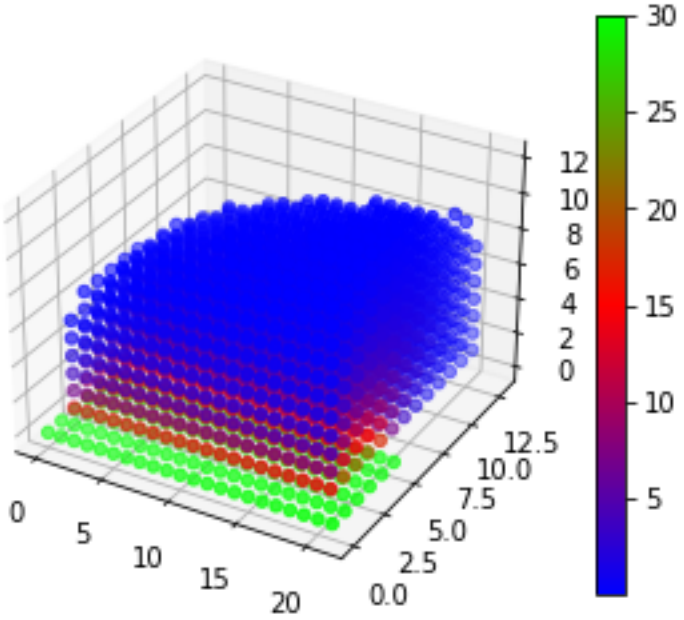

Figure 5.13 3D plot showing the model with an edge heat source

5.2.4 Summary

Table 5.2 summarizes the results of the two-dimensional model tests. The phase boundary location notes the farthest melted node (out of 20) - however, since this is the two-dimesional model, this does not necessarily mean that the entire vertical line of nodes at that location is melted. Instead, this location is the farthest protruding node of the phase boundary, out of 20 nodes.

Alpha Value	Latent Heat (kJ/kg)	Initial Temp	Phase Boundary Loc
0.01	100	$10°C$	9
0.1	100	$10°C$	8
0.3	100	$10°C$	8
0.5	100	$10°C$	8
0.7	100	$10°C$	8
0.99	100	$10°C$	7
0.5	11.4	$10°C$	18
0.5	23	$10°C$	14
0.5	105	$10°C$	8
0.5	184	$10°C$	6
0.5	293	$10°C$	4
0.5	334	$10°C$	4
0.5	100	$1°C$	4
0.5	100	$50°C$	20
0.5	100	$100°C$	20

Table 5.2 Summary of parameter comparisons for the two-dimensional model.

CHAPTER SIX

CONCLUSIONS

To begin, we derived the one-phase one-dimensional Stefan problem. First, we established some information about enthalpy and latent heat, which provided context for the complexity of the problem. We then explored some characteristics of the classic Stefan problem, including some parameters for the analytical solution, as well as the existence and uniqueness of the solution.

We then stated the two-phase and two-dimensional Stefan problems, highlighting the motivation for finding a numerical model for solving.

Next, we discussed fractional operators in Chapter 3. We established important properties of fractional derivatives, highlighting the differences between Riemann-Liouville and Caputo and their uses in differential equations. With a few proofs, we were able to conclude that the Caputo derivative would be the most useful for our Stefan model.

In Chapter 4, we outlined our Stefan Caputo model in both one and two dimensions. We worked through the finite difference discretization for the fractional operator, as well as the successive over-relaxation (SOR) method for solving.

The results of our model were outlined in Chapter 5. After first showing that our model matched the analytical solution for specific parameters, we moved on to test for unknown solutions. We ran dozens of tests, looking at the melting rate for different parameters - alpha values, latent heat, and initial temperature. For the two-dimensional model, we also experimented with shifting the location of the heat source concentration, showing how the melting pattern shifted with it.

This successful model has shown that the Caputo fractional derivative, with our finite difference discretization and SOR method, can be used to model the Stefan problem in one and two dimensions. Our model is general enough that parameters can be easily changed based on the type of material or heat source, making it useful for experimetation.

Further work on this model would be beneficial. There are a number of different paths to take, such as

1. Implementing the model in higher dimensions
2. Optimizing the code or using other methods to decrease processing time, allowing for larger scale tests
3. Increasing the model to two phases
4. Applying fractional operators to other free boundary problems, or to other PDE/ODEs

REFERENCES

[1] N. H. Abel. "Solution of a couple of problems by means of definite integrals (FR)". In: *Magazin for Naturvidenskaberne* (1823), pp. 55–68.

[2] Abdon Atangana. *Fractional Operators with Constant and Variable Order with Application to Geo-Hydrology*. Academic Press, 2018.

[3] G. et. al Benenti. "Non-Fourier heat transport in nanosystems". In: *La Rivista del Nuovo Cimento* (2023).

[4] Marek Błasik and Malgorzata Klimek. "Numerical solution of the one phase 1D fractional Stefan problem using the front fixing method". In: *Mathematical Methods in the Applied Sciences* 38 (Nov. 2014).

[5] V. Bokil and N. Gibson. *Finite Difference, Finite Element and Finite Volume Methods for the Numerical Solution of PDEs*. Presentation Oregon State University. 2007.

[6] Michele Caputo. "Linear model of dissipation whose Q is almost frequency independent. II". In: *Geophysical Journal Internationl* 13.5 (1967), pp. 529–539.

[7] L. Debnath. "Fractional integral and fractional differential equations in fluid mechanics". In: *Fractional Calculus and Applied Analysis* 6.2 (2003), pp. 119–155.

[8] Hu H. Du M. Wang Z. "Measuring memory with the order of fractional derivative". In: *Sci Rep* (2013).

[9] Avner Friedman. *Partial Differential Equations of Parabolic Type*. 2008.

[10] D.M. Gordievskikh and P.N. Davydov. "Numerical solution of some degenerate differential equations with fractional time derivative". In: *NAUKOVEDENIE* 7, NO. 2 (2015).

[11] R. Gorenflo and F. Mainardi. *Fractional Calculus: Integral and Differential Equations of Fractional Order*. 2000.

[12] M. Greenberg. *Foundations of Applied Mathematics*. Prentice-Hall Inc., 1978.

[13] R. Hinrichs and P. Urone. *Physics by OpenStax*. OpenStax, 2020.

[14] M. K. Ishteva. *Properties and Applications of the Caputo Fractional Operator*. 2005.

[15] C. Johnson. *Numerical Solution of Partial Differential Equations by the Finite Element Method*. Dover, 1987,2009.

[16] Tobias Jonsson. *On the one dimensional Stefan problem with some numerical analysis*. Bachelor's Thesis. 2013.

[17] A. A. LACEY and A. B. TAYLER. "A Mushy Region in a Stefan Problem". In: *IMA Journal of Applied Mathematics* 30.3 (May 1983), pp. 303–313.

[18] R. LeVeque. *Finite Difference Methods for Ordinary and Partial Differential Equations*. Society for Industrial and Applied Mathematics, 2007.

[19] I. Podlubny. *Fractional Differential Equations: An Introduction to Fractional Derivatives, Fractional Differential Equations, to Methods of Their Solutions and Some of their Applications*. Academic Press, 1998.

[20] G. W. Recktenwald. "Finite-Difference Approximations to the Heat Equation". In: (2011).

[21] Sabrina D. Roscani, Nahuel D. Caruso, and Domingo A. Tarzia. "Explicit solutions to fractional Stefan-like problems for Caputo and Riemann–Liouville derivatives". In: *Communications in Nonlinear Science and Numerical Simulation* 90 (2020), p. 105361.

[22] Henry S.H. Shaw. *Investigation of the nature of surface resistance of water and of stream-line motion under certain experimental conditions.* Inst. N.A. London, 1898.

[23] M.I. University of Oxford. "Free Boundary Problems". In: *Continuum Methods for Industry* ().

[24] D. Young. *Iterative Solution of Large Linear Systems*. Academic Press, 1971.

[25] David M. Young. "Iterative methods for solving partial difference equations of elliptical type". PhD thesis. Harvard University, 1950.

APPENDICES

APPENDIX A

Block Diagram for One-Dimensional Algorithm

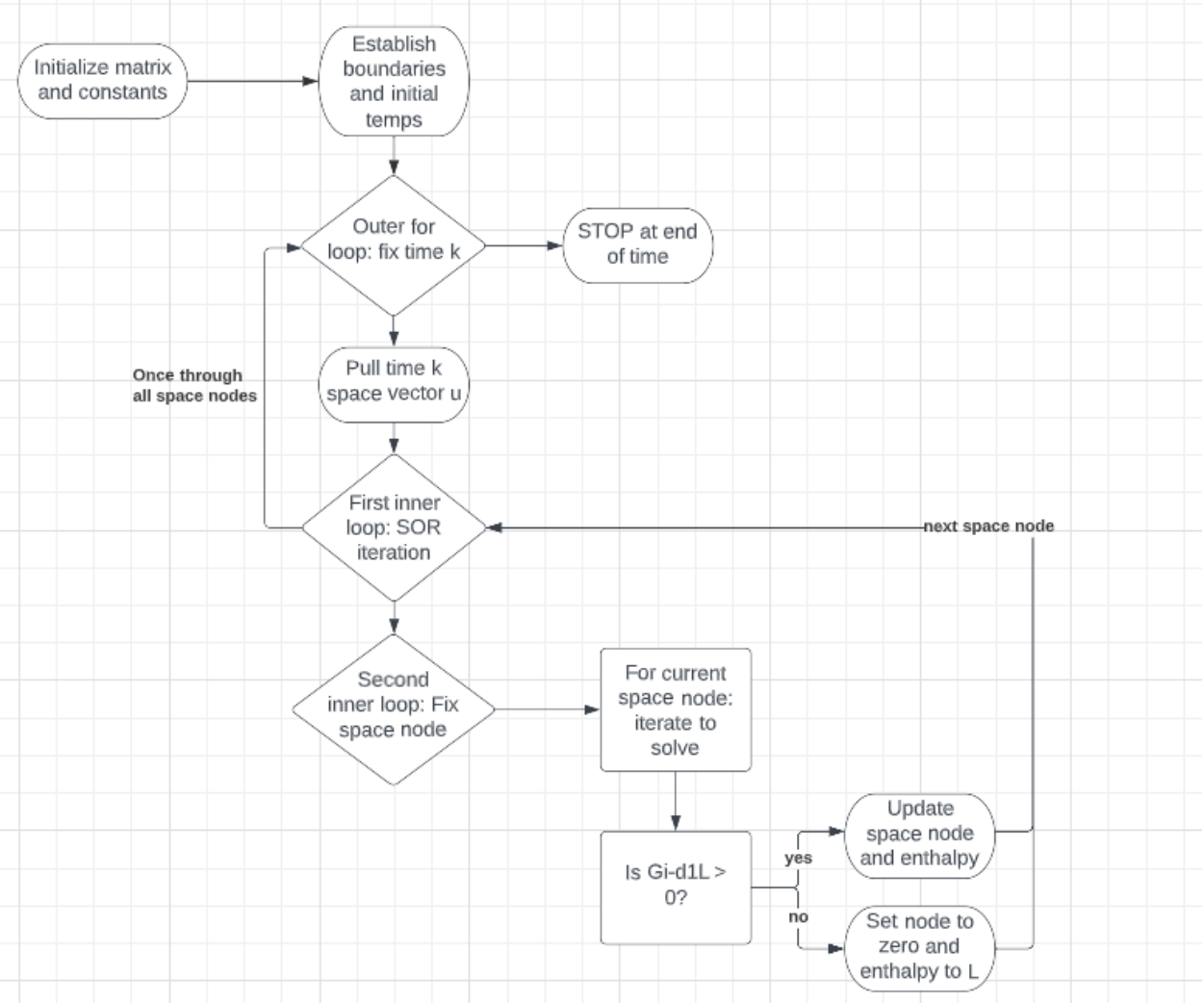

Figure A.1 Block diagram depicting the algorithm for the one-dimensional Stefan-Caputo model

APPENDIX B

Code for One-Dimensional Stefan Caputo Model

```
import numpy as np
from scipy.special import gamma, factorial
import matplotlib.pyplot as plt
from matplotlib.ticker import MultipleLocator
import math

#variable definitions



def stefan_caputo(time, space, alpha, temp, latent):
    t=time #time nodes
    m=space #space nodes
    alpha=alpha #fractional constant
    t8=temp #heat source temp
    l=latent heat #latent heat
    h=1/m #space intervals
    tau=1/t #time intervals
    eps=h**2 #sor condition
    ro=1 #per unit
    cs=1.7
    k=4.1869
    u=np.zeros((t+2,m+2)) #temperature matrix
    sum1=np.zeros((1,m+2)) #temporary sum
```

```
enthalpy=np.zeros((t+2,m+2)) #enthalpy matrix
sigma=1.7 #sor parameter
r=np.zeros((t+2,m+2)) #error calculation matrix
# filling in the first column with the heat source temp
for tk in range(0,t+2):
    u[tk,0]=t8
for tk in range(1,t+1): #time loop
    sum1 = np.zeros((1,m+2))
    for j in range(1,m+1):
        for i in range(1,tk-1): #temporary loop - calculating changes
            sum1[0,j]=sum1[0,j]+enthalpy[tk-i,j]*(2*i**(1-alpha)-(i-1)
                ↪ **(1-alpha)-(1+i)**(1-alpha))
    s=eps+1

    while (s>eps): #sor condition
        for j in range(1,m+1): #space loop
            summ=sum1[0,j]+((1-sigma)*u[tk,j]+(u[tk,j-1]+u[tk,j+1])*sigma
                ↪ /2)*2*(tau**alpha)*gamma(2-alpha)/(sigma*h*h)
            if summ<=l*ro or summ==0: #adjust enthalpy but keep temp at 0
                enthalpy[tk,j]=summ
                u[tk,j]=0
            else: #melted
                u[tk,j]=((1-sigma)*u[tk,j]+sigma*h*h*(sum1[0,j]-l*ro)/(2*(
                    ↪ tau**alpha)*gamma(2-alpha))+(u[tk,j-1]+u[tk,j+1])*
                    ↪ sigma/2)/(1+k*sigma*h*h/(2*(tau**alpha)*gamma(2-
                    ↪ alpha)))
```

```
                enthalpy[tk,j]=k*u[tk,j]+l*ro
        s=0
        for j in range(1,m+1):
            summ=enthalpy[tk,j]-sum1[0,j]
            r[tk,j]=((2*u[tk,j]-u[tk,j-1]-u[tk,j+1])/h**2) + summ/((tau**
                ↪ alpha)*gamma(2-alpha))
            s=s+(r[tk,j]**2)
        s=np.sqrt(s)
    return u


def plot_stefan_caputo(u, color):
    #plotting - remove unmelted nodes
    u=np.delete(u, 1, 0)
    y2=np.array([])
    x2=np.array([])

    for k in range(0,t-1):
        add=0
        x2=np.append(x2,k)
        for n in range (0,m):
            if u[k,n]>0:
                add=add+1
        y2=np.append(y2,add)
    plt.figure(k)
    plt.xlabel("Time")
    plt.ylabel("Space␣Coordinates␣Melted")
```

```
plt.plot(x2,y2, color=color)
```

APPENDIX C

Code for Two-Dimensional Stefan Caputo Model

```
import numpy as np
from scipy.special import gamma, factorial
import matplotlib.pyplot as plt
from mpl_toolkits.mplot3d import Axes3D

m=20 #space
t=20 #time


def stefan_caputo_2d(time, space, alpha, latent):
    t=time #time nodes
    m=space #space nodes
    alpha=alpha #fractional alpha value
    l=latent #latent heat constant
    h=1/m #space intervals
    tau=1/t #time intervals
    eps=h**2 #sor condition
    t8=10 #initial heat source temp
    ro=1
    cs=1.7
    k=4.1869
    u=np.zeros((t+2,m+2,m+2)) #temperature matrix
```

```
enthalpy=np.zeros((t+2,m+2,m+2)) #enthalpy matrix
sigma=1.7 #sor parameter
for tk in range(0,t+2):
    for j in range(0,t+2):
        u[tk,j,0]=t8
for tk in range(1,t+1):
    sum1=np.zeros((m+2,m+2))
    for v in range(1,m+1):
        for j in range(1,m+1):
            for i in range(1,tk-1):
                sum1[v,j]=sum1[v,j]+enthalpy[tk-i,v,j]*(2*i**(1-alpha)-(i
                    ↪ -1)**(1-alpha)-(i+1)**(1-alpha))
        s=eps+1
        while(s>eps):
            for i in range(1,m+1):
                for j in range(1,m+1):
                    summ=sum1[i,j]+((1-sigma)*u[tk,i,j]+(u[tk,i-1,j]+u[tk,
                        ↪ i+1,j]+u[tk,i,j-1]+u[tk,i,j+1])*sigma/4)*4*(tau
                        ↪ **alpha)*gamma(2-alpha)/(sigma*h**2)
                    if summ<=l*ro or summ==0:
                        enthalpy[tk,i,j]=summ
                        u[tk,i,j]=0
                    else:
                        u[tk,i,j]=((1-sigma)*u[tk,i,j]+sigma*h**2*(sum1[i,
                            ↪ j]-l*ro)/(4*(tau**alpha)*gamma(2-alpha))+(u[
                            ↪ tk,i-1,j]+u[tk,i+1,j]+u[tk,i,j-1]+u[tk,i,j
```

```
                        ↪ +1])*sigma/4)/(1+k*sigma*h**2/(4*(tau**alpha
                        ↪ )*gamma(2-
    alpha)))
                    enthalpy[tk,i,j]=ro*k*u[tk,i,j]+l*ro
            s=0
            for i in range(1,m+1):
                for j in range(1,m+1):
                    summ=enthalpy[tk,i,j]-sum1[i,j]
                    r=(4*u[tk,i,j]-u[tk,i-1,j]-u[tk,i+1,j]-u[tk,i,j-1]-u[
                        ↪ tk,i,j+1])/(h**2)+summ/(tau**alpha*gamma(2-alpha
                        ↪ ))
                    s=s+r**2
            s=np.sqrt(s)



stefan_caputo_2d(20, 20, 0.5, 334)


u[u==0]=np.nan


x = np.indices(u.shape)[0]
y = np.indices(u.shape)[1]
z = np.indices(u.shape)[2]
col = u.flatten()


# 3D Plot
```

```
fig = plt.figure()

ax3D = fig.add_subplot(projection='3d')

cm = plt.colormaps['brg']

p3d = ax3D.scatter(x, y, z, c=col, cmap=cm)

plt.colorbar(p3d)


plt.show()
```